



Dosimetric Anchoring of *In Vivo* and *In Vitro* Studies for Perfluorooctanoate and Perfluorooctanesulfonate

Journal:	<i>Toxicological Sciences</i>
Manuscript ID:	TOXSCI-13-0528.R1
Manuscript Type:	Research Article
Date Submitted by the Author:	09-Aug-2013
Complete List of Authors:	Wambaugh, John; United States Environmental Protection Agency, National Center for Computational Toxicology Setzer, R.; USEPA, Mail Drop B143-05 Pitruzzello, Ann; Research Triangle Institute, Liu, Jie; USEPA, Mail Drop B143-05 Reif, David; US EPA, National Center for Computational Toxicology Kleinstreuer, Nicole; U.S. Environmental Protection Agency, Office of Research and Development, National Center for Computational Toxicology Wang, Nina; EPA/ORD/NCEA, Sipes, Nisha; U.S. Environmental Protection Agency, Office of Research and Development/National Center for Computational Toxicology Martin, Matthew; US EPA, Das, Kaberi; USEPA, Mail Drop B143-05 DeWitt, Jamie; East Carolina University, Pharmacology and Toxicology; Strynar, Mark; USEPA, Mail Drop B143-05 Judson, Richard S.; US EPA, National Center for Computational Toxicology Houck, Keith; USEPA, NCCT Lau, Christopher; US Environmental Protection Agency, Toxicity Assessment Division
Key Words:	perfluorinated agents < Agents, pharmacokinetics < Biotransformation and Toxicokinetics, alternatives to animal testing < In Vitro and Alternatives, biological modeling < Risk Assessment, dosimetry < Risk Assessment
Society of Toxicology Specialty Section Subject Area:	Biological Modeling [103]

Dosimetric Anchoring of *In Vivo* and *In Vitro* Studies for Perfluorooctanoate and Perfluorooctanesulfonate

John F. Wambaugh^{a,1}, Woodrow Setzer^a, Ann M. Pitruzzello^b, Jie Liu^a, David Reif^a,
Nicole Kleinstreuer^a, Nina Ching Y. Wang^c, Nisha Sipes^a, Matthew Martin^a, Kaberi Das^d,
Jamie DeWitt^e, Mark Strynar^f, Richard Judson^a, Keith Houck^a, and Christopher Lau^d

^aNational Center for Computational Toxicology,
^dNational Health and Environmental Effects Research Laboratory,
^fNational Exposure Research Laboratory,
Office of Research and Development, U.S. Environmental Protection Agency, Research
Triangle Park, North Carolina 27711

^bResearch Triangle Institute, Research Triangle Park, North Carolina 27711

^cNational Center for Environmental Assessment
Office of Research and Development, U.S. Environmental Protection Agency,
Cincinnati, Ohio, 45268

^eDepartment of Pharmacology and Toxicology, Brody School of Medicine, East Carolina
University, Greenville, North Carolina 27834

¹**Corresponding Author:**
Mail Code B205-1
109 T.W Alexander Dr, NC 27711, USA
Wambaugh.john@epa.gov
Phone: (919) 541-7641; fax: (919) 541-1194

Abstract

In order to compare between *in vivo* toxicity studies, dosimetry is needed to translate study-specific dose regimens into dose metrics such as tissue concentration. These tissue concentrations may then be compared with *in vitro* bioactivity assays to perhaps identify mechanisms relevant to the lowest observed effect level (LOEL) dose group and the onset of the observed *in vivo* toxicity. Here we examine the perfluorinated compounds (PFCs) perfluorooctanoate (PFOA) and perfluorooctanesulfonate (PFOS). We analyzed nine *in vivo* toxicity studies for PFOA and thirteen *in vivo* toxicity studies for PFOS. Both PFCs caused multiple effects in various test species, strains, and genders. We used a Bayesian pharmacokinetic (PK) modeling framework to incorporate data from six PFOA PK studies and two PFOS PK studies (conducted in three species) to predict dose metrics for the *in vivo* LOELs and no observed effect levels (NOELs). We estimated PK parameters for eleven combinations of chemical, species, strain, and gender. Despite divergent study designs and species-specific PK, for a given effect we found that the predicted dose metrics corresponding to the LOELs (and NOELs where available) occur at similar concentrations. *In vitro* assay results for PFOA and PFOS from EPA's ToxCast project were then examined. We found that most *in vitro* bioactivity occurs at concentrations lower than the predicted concentrations for the *in vivo* LOELs, and higher than the predicted concentrations for the *in vivo* NOELs (where available), for a variety of non-immunological effects. These results indicate that given sufficient PK data, the *in vivo* LOELs dose regimens, but not necessarily the effects, could have been predicted from *in vitro* studies for these two PFCs.

Key Words: perfluorooctanoate (PFOA); perfluorooctanoic acid (PFOA); perfluorooctanesulfonate (PFOS); perfluorooctanesulfonic acid (PFOS); compartment model; saturable resorption model; pharmacokinetics; statistical analysis; Bayesian analysis; ToxCast; in vitro-in vivo extrapolation

INTRODUCTION

In vivo toxicity studies are often characterized by the no observed effect level (NOEL) and/or the lowest observed effect level (LOEL) dose groups for a given toxic outcome (Martin *et al.*, 2009). Even if the pharmacodynamic mechanism is conserved, comparing LOELs between studies is confounded by differences in pharmacokinetics, which can be not only biological in origin (*e.g.* species, gender) but also due to dose regimen (*e.g.* spacing, magnitude, duration, and route of administration). If, however, the test compound activates a consistent mode of action across studies, then somewhere between the NOEL and the LOEL, the tissue concentrations must be sufficient to perturb that mechanism in a statistically significant number of test animals (Allen *et al.*, 1994). If that mode of action is conserved in humans, then the chemical exposures that might cause these effects in humans may be inferred (Boobis, 2010).

The U.S. Environmental Protection Agency (EPA)'s ToxCast study comprises hundreds of high-throughput, chiefly *in vitro* assays investigating a large number of chemicals, including perfluorinated compounds (PFCs) (Judson *et al.*, 2010; Reif *et al.*, 2010). Known chemical toxicants have been examined in ToxCast in order to develop *in vitro* signatures of chemical toxicity for application to chemicals with little or no *in vivo* toxicological data (Kleinstreuer *et al.*, 2011; Knudsen and Kleinstreuer, 2011; Martin *et al.*, 2011; Sipes *et al.*, 2011). These signatures of toxicity are developed by correlating observed *in vitro* activity – positive assay results –with actual *in vivo* toxicity (Blaauboer, 2010).

In order to interpret *in vitro* assay bioactivity the biochemical perturbation characterized by that assay and the *in vivo* context of that perturbation must be identified (Judson *et al.*, 2011). If the *in vitro* concentrations that cause activity are consistent with the transition region from NOEL to LOEL *in vivo*, then an empirical association may exist between that *in vitro* activity and the observed *in vivo* toxicity. We hypothesize that those assays that are consistent with the transition from NOEL to LOEL in many *in vivo* studies may help to identify the underlying mechanism of toxicity.

Here, we use two PFCs – perfluorooctanesulfonate (PFOS) and perfluorooctanoate (PFOA) – as model chemicals for comparing *in vivo* toxicity and *in vitro* bioactivity. PFCs are long chain fatty acid analogs with fluorine atoms in the place of all hydrogen atoms. Among the ToxCast chemicals, PFOS and PFOA are of particular interest because measurable levels are detected in the general population of the United States (Calafat *et al.*, 2007; Olsen *et al.*, 2012) and elsewhere in the world (Harada *et al.*, 2010; Haug *et al.*, 2009). PFOS and PFOA are relatively well studied chemicals; toxicity studies with PFOS and PFOA in adult rodents and monkeys have documented LOELs for liver effects and maternal LOELs for developmental endpoints in offspring (Lau *et al.*, 2007; Lau *et al.*, 2004).

The pharmacokinetics (PK) of PFOA is known to be non-linear (Andersen *et al.*, 2006; Lou *et al.*, 2009), and the half-life for elimination from the body can vary between species and genders by many orders of magnitude (Lau, *et al.*, 2007). In occupationally exposed workers the elimination half-life has been estimated to be from 2.3 to 3.8 years (Bartell *et al.*, 2010; Olsen *et al.*, 2007). The long human half-lives are in contrast to hours for female rats, days for male rats, and weeks for mice, and about a month for monkeys (Lau, *et al.*, 2007). The PK behavior of PFOS is less studied but has been modeled as being generally similar to that of PFOA (Andersen, *et al.*, 2006; Chang *et al.*, 2012).

This study has two major goals: First, we wish to examine the concordance of various measures of internal exposure for the available toxicological *in vivo* studies. This meta-analysis of nine PFOA and thirteen PFOS studies is performed using PK data drawn from six PFOA and two PFOS PK *in vivo* studies. The PK data are analyzed within a Bayesian framework that allows prediction across species, strains, and genders, in order to identify consistent measures of exposure, *i.e.* dosimetric anchors.

Second, we evaluate the correlation between these *in vivo* effects and observed *in vitro* activities. Recently Aylward and Hayes (2011) have noted general concordance between the *in vitro* activation concentrations and the serum concentrations at the end

of toxicity studies. For metabolizing enzymes, Bjornsson *et al.* (2003) described a heuristic for extrapolation of *in vitro* bioactivities to possible or likely *in vivo* activity; here we extend this comparison between a range of *in vitro* bioactivities (the ToxCast assay suite) with *in vivo* serum concentration time-courses.

METHODS AND MATERIALS

Data Sources

1. In Vivo Toxicity Data Sets

Toxicity data including study design, LOELs and, where available, NOELs from nine PFOA studies and thirteen PFOS studies are summarized in Tables 1 and 2, respectively. Toxicity endpoints were categorized as liver, thyroid, developmental, reproductive, or immunological. Where available, serum values at study termination are also reported.

2. Pharmacokinetic Data Sets

For each species/strain/gender combination that was considered, a single distribution of parameters was determined that should be most consistent with all the available data.

PFOA PK was modeled for three species: cynomolgus monkeys (Butenhoff *et al.*, 2004b), Sprague Dawley rats (Kemper, 2003), and two strains of mice. The data from the two strains of mice were separately analyzed: CD1 (Lou, *et al.*, 2009) and C57Bl/6 (DeWitt *et al.*, 2008). Due to the pronounced difference in the PK of male and female rats for PFOA, the two genders were fit separately. Since a significant gender difference has not been observed in mice and more female data were available (Lou, *et al.*, 2009), only the female data were used. For monkeys, the majority of data were for males; however a small amount of data were used from experiments on both male and female monkeys that were administered compound intravenously (iv). The female data were

analyzed with the assumption that the only difference between the genders for monkey was body weight (BW) (the half-life in monkeys is believed to be only slightly different between genders). The PFOA PK data are summarized in Table 3.

PFOS PK was modeled for three species: cynomolgus monkeys (Chang, *et al.*, 2012; Seacat *et al.*, 2002), Sprague Dawley rats (Chang, *et al.*, 2012), and CD1 mice (Chang, *et al.*, 2012). The PFOA PK data are summarized in Table 4.

3. ToxCast In Vitro Data

The pilot (Phase I) of the ToxCast program measured the activity of 309 compounds, including PFOA and PFOS, against a suite of *in vitro* assays provided by separate vendors using different technologies including cell-based and biochemical (cell-free) assays. Most chemical-assay combinations were run in concentration-response format and from each concentration-response curve it was determined statistically whether the chemical was active or not. If found active, a characteristic concentration (AC_{50} – the concentration at which 50% of maximum activity was seen) and maximum efficacy (E_{max}) were determined. The data are described in Judson *et al.* (2009). All data and additional assay information are available from the ToxCast web site (<http://www.epa.gov/ncct/toxcast>) and from the Aggregated Computational Toxicology Repository (<http://www.epa.gov/actor/>).

Results from three ToxCast technology platforms in which PFOS and PFOA were active are reported here. The first, contracted from Attagene, Inc. (Research Triangle Park, NC) (www.attagene.com), consisted of two highly multiplexed assays; one with 48 human transcription factor DNA-binding sites controlling reporter gene expression (denoted CIS) and the other with 25 human nuclear receptor (NR) superfamily members using a mammalian 2-hybrid, GAL4 system (TRANS) (Martin *et al.*, 2010), both in the HepG2 human hepatoma cell line. The second platform, contracted from BioSeek, Inc. (South San Francisco, CA) (www.bioseek.com), used the biologically multiplexed activity profiling (BioMAP) platform for assaying cellular signaling pathways in complex,

co-cultured, primary human cell systems (Houck *et al.*, 2009). The third, contracted from NovaScreen (Hanover, MD) (www.caliperls.com), was an array of 292 biochemical assays including receptor binding and enzyme inhibition (Knudsen *et al.*, 2011).

The efficacy (E_{max}) and potency (inverse of AC_{50}) for all active assays are shown in Figure 1. Efficacy was scaled by a fold-change or percent activity cutoff that depended upon the variability of the specific assay technology; a dose-response curve with a scaled efficacy of one would be at the cutoff and therefore filtered for not showing a significant change over background. For PFOA there were 12 active ToxCast assays, while PFOS was more promiscuous, with 52 assays indicating activity. The three assays common to both PFOS and PFOA are described in Table 5 and discussed further in the Results section. Descriptions of all assays activated by either PFOS or PFOA are given in Supplemental Table 2.

In Figure 1 five PFOS assays are only marginally above the assay cutoff: BSK_BE3C_PA11_down, BSK_3C_SRB_down, and BSK_BE3C_hLADR_down for the BioSeek technology and NVS_ENZ_hAKT2, and NVS_ENZ_hGSK3b for the NovaScreen technology (see Supplemental Table 2 for assay descriptions). For PFOA the BioSeek BSK_SM3C_SAA_up assay is only marginally above the cutoff.

Pharmacokinetic Model

The PK model for PFCs (depicted in Figure 2) was adapted with minor modifications from Andersen *et al.* (2006). The primary parameters are defined in the caption of Figure 2. The salient feature of the Andersen *et al.* (2006) model is that the free concentration of PFCs in the central compartment (given by $free \cdot C_1$) is cleared to a filtrate compartment where it is either excreted or resorbed via a saturable process with a Michaelis-Menten form. The Andersen *et al.* (2006) model was modified to include a gut compartment from which PFCs were absorbed using a first order rate constant k_a .

The flow through the filtrate (Q_{fil}) is determined by multiplying a fraction (Q_{filc}) times the cardiac output, which is scaled by BW to the power 0.74. Only the free chemical in the central compartment ($free \cdot C_1$) flows to the filtrate. The volume of the central compartment (V_c) and the volume of the filtrate (V_{fil}) are determined by respectively multiplying BW by the fractions V_{cc} and V_{filc} , respectively. The flow between the central and secondary compartments (Q_d) is determined from multiplying V_c by the rate of flow from the central compartment to the second (k_{12}). The maximum rate of the saturable resorption Michaelis-Menten kinetics ($T_{maximum}$) is scaled by multiplying a constant (T_{maxc}) by BW.

In the original Andersen *et al.* (2006) analysis, the deep tissue (secondary) compartment was characterized in terms of the rates to and from that compartment (k_{12} and k_{21} , respectively). This corresponds to a volume of distribution $V_2 = k_{12} \cdot V_1 / k_{21}$, so that the ratio of the volume of the second compartment to the first, $R_{v2:v1} = k_{12} / k_{21}$. The original model was modified to enforce the assumption that the primary (serum) compartment contains a significant portion of the PFCs: the volume of distribution the deep tissue compartment was constrained to be no more than 100 times greater than the volume of the serum – in effect this is an upper limit on the fraction of PFCs sequestered within tissue. For this reason the ratio of the two volumes is estimated, rather than the rate from the second compartment to the first compartment. The rate of flow from the deep tissue back to the serum was calculated as $k_{21} = k_{12} / R_{v2:v1}$.

The model was implemented using R (version 2.10.0, (R Development Core Team, 2012)) and solved with the deSolve package (version 1.5, (Soetaert *et al.*, 2010)).

Bayesian Analysis

1) Statistical Model

A non-hierarchical model for parameter values was assumed; *i.e.* there is a single value shared by all individuals of the same species/strain (with rat further subdivided by gender). BW and treatment (number and magnitude of doses) are the only parameters

that may vary between individuals; however, with the exception of the Kemper (2003) data, individual BWs were not available so that an average BW was determined for each combination of species and gender. Measurement errors were assumed to be log-normally distributed, with each combination of study and tissue type having a separate measurement standard deviation that was estimated as part of the statistical analysis.

2) *Sampler*

Bayesian analysis was performed using Markov Chain Monte Carlo (MCMC) (Gelman *et al.*, 2004). The MCMC sampler, implemented as an R package, was developed and used by Garcia *et al.* (Garcia *et al.*). The Metropolis-Hastings algorithm (Hastings, 1970; Metropolis *et al.*, 1953) was used to find the posterior distributions for each parameter such that the predictions of the PK model are consistent with the data and the prior assumptions. A multivariate proposal distribution for the PK parameters and measurement variances was determined from several initial runs starting with the Lou *et al.* (2009) CD1 mouse PK values and a diagonal, *i.e.* uncorrelated, proposal distribution.

3) *Priors*

Bayesian analysis allows formal inclusion of prior knowledge in the form of set distributions on the parameters being estimated (Gelman, *et al.*, 2004); however, that empirical PK parameters can have a wide range of plausible values. (Wambaugh *et al.*, 2008). We chose vague, bounded prior distributions that are intended to be significantly informed by the data. For all estimated parameters the prior knowledge was assumed to be distributed log-normally. This constrained the parameters to positive values. The mean and variances assumed for the CD1 mice, male and female Sprague-Dawley rats, and Cynomolgus monkeys are given in Supplemental Table 1. For the analysis of PFOA in C57Bl/6 mice the available data were insufficient to achieve a converged statistical analysis, so the posterior parameter distributions for the CD1 mouse, with the variances increased ten-fold, were used as a prior. The priors for measurement variances were uniform between 0 and 5.

4) *Convergence*

1
2
3 The crux of a Bayesian analysis is assessing whether the distributions of values in the
4 Markov Chain reflect the posterior distributions of the statistical model given the priors
5 and the data. Each distribution of parameter values was considered to be “burned in”
6 (*i.e.*, drawn from the true posterior and independent of the assumed starting values)
7 when they passed the Heidelberger and Welch stationarity test (Heidelberger and
8 Welch, 1983) as implemented in the Convergence Diagnosis and Output Analysis
9 Software for Gibbs sampling output (CODA) Package (Best *et al.*, 1995) for R.
10
11
12
13
14
15
16

17 *Predicted Dose Metrics*

18 Using these appropriately parameterized PK models for serum as a function of dose
19 and time, a variety of predictions can be made. For each study with a toxicological
20 endpoint and LOEL, the time-integrated serum concentration (area under the curve or
21 AUC), average serum concentration, and maximum serum concentration were
22 determined over the course of the *in vivo* study. All dose metrics were calculated using
23 the total serum concentration of compound. Generally, it was assumed that animals
24 were observed at the end of dosing. However, for the Butenhoff *et al.* (2009) PFOS
25 study two different AUCs were calculated – gestational only (for the male offspring
26 endpoint) and gestational plus twenty days postnatal (for the maternal endpoint). This
27 separation of the two exposures neglects lactational transfer of compound, which was
28 not modeled. For many of the *in vivo* studies a serum concentration at euthanasia was
29 measured, and for these studies a final serum concentration was predicted at the time
30 corresponding to euthanasia.
31
32
33
34
35
36
37
38
39
40
41
42
43

44 For each estimated PK parameter, MCMC produces a series of values that, taken as a
45 whole, represent the distribution of parameter values consistent with the data and the
46 priors. These parameter distributions can in turn be used to generate distributions of
47 predictions, *e.g.* average serum concentration or AUC. If there is large parameter
48 uncertainty for parameters that greatly influence the predicted value, then the
49 distribution of predicted values will be wide. If the quantity being predicted is not
50 sensitive to the uncertain parameter, then the distribution of the predicted value will be
51
52
53
54
55
56
57
58
59
60

unaffected. Assessing parameter uncertainty allows appropriate confidence in model predictions.

Determination of Transition Concentrations

The distributions of PK predictions were used to demark the transition region from NOEL to LOEL, *i.e.* the region of predicted dose metrics containing the lowest chemical dose that causes an observable toxic effect. The transition region for each *in vivo* study treatment is bounded by the upper 95% confidence value of the distribution of average serum concentrations calculated for the LOEL and, if available, the lower 95% confidence value for the NOEL. If no NOEL was available an arbitrary lower value, LOEL/100, was used.

When multiple *in vivo* studies examined the same toxicity endpoints, the transition regions from the studies can be used jointly to further refine the transition region. Transition regions were calculated in two ways: the intersection of all studies for a given chemical and toxicity was more restrictive, using the highest NOEL and the lowest LOEL; while the union of all studies was broader in that the lowest NOEL and the highest LOEL was used. In some cases the exposures calculated for the *in vivo* studies conflicted, producing a NOEL in one study in excess of the LOEL in the other study. In this case no intersecting transition region was identified and only the union region was available.

Determination of Benchmark Dose (BMD)

For a three PFOA studies where there was no NOEL dose group but the effect per dose group data were available, a benchmark dose was estimated using the U.S. EPA Benchmark Dose Software v2.3.1.

RESULTS

Nine PFOA *in vivo* studies and thirteen PFOS *in vivo* studies were examined for monkeys, rats, and two strains of mice, in some cases for separate genders. We

1
2
3 predicted dose metrics, including the average serum concentration, for the LOEL dose
4 group for each endpoint in each study and, where available, the NOEL dose group. For
5 many of the PFOA studies a NOEL group was lacking (*i.e.* the lowest dose tested
6 showed an effect), and for three of these no NOEL study-endpoint combinations there
7 was sufficient data were available to perform a benchmark dose analysis.
8
9
10
11
12

13 14 **Analysis of *in vivo* PK data sets**

15
16
17 In the absence of ideal PK data for either PFOS or PFOA, a range of possible PK model
18 predictions that were equally consistent with the data were generated with Bayesian
19 statistical analysis. Each dose metric predicted from this analysis has a distribution of
20 values consistent with the data which we describe by a mean or median value and 95%
21 credible interval; broader distributions reflect greater uncertainty.
22
23
24
25
26
27

28 Model predictions were assessed by comparing the predicted final serum concentration
29 for each treatment with any measured final serum concentration in the *in vivo* toxicity
30 experiments. The predictions (Figure 3) were generally similar to the measurements
31 (within a factor of two). There were no systematic differences in the performance of the
32 predictions for different species, genders, and strains despite the different PK data sets
33 used. In Figure 3 the credible intervals are smaller than the scatter of the points around
34 the perfect predictor (1:1) line – since these predictions do not perfectly match the
35 measured serum concentrations, there remains uncertainty about the PK behavior that
36 has not been fully characterized. The specific predicted values are reported in
37 Supplemental Tables 3-6.
38
39
40
41
42
43
44
45
46

47 Since the uncertainty of the parameters depends on the amount of available data, it is
48 unsurprising that the distributions of parameter values are larger for those test animals
49 with less data (Table 3 and Table 4). Since most of the available PK studies were not
50 designed to probe non-linear phenomena (*e.g.* saturable resorption), parameters
51 describing the saturable resorption process are especially uncertain. These parameters
52 have been difficult to estimate in previous studies (Andersen, *et al.*, 2006; Lou, *et al.*,
53
54
55
56
57
58
59
60

2009). However, the form of the saturable resorption model seems to be an appropriate empirical description of the PK for PFCs (Lou, *et al.*, 2009). Time course plots comparing the predictions for the median parameter values and the data used for estimating the parameters are available in Supplemental Figures 1-13.

1) PFOA PK parameters

The estimated PK parameters (median and 95% interval) for PFOA are presented in Table 6. The parameter distributions generally appear biologically plausible: the median fraction of blood flow to the filtrate (Q_{filc}) was physiologically consistent and plausible (*i.e.* less than or equal to the fraction of blood flow to the kidney) in all cases, but the uncertainty, as characterized by 95% credible interval, was quite large in some cases.

Parameters for PFOA in male and female rats were similar, including the affinity of the putative resorption transporters, except that the maximum Michaelis-Menten transport rate was nearly two hundred times greater for the males. This potentially corresponds to differences in either the expression of the relevant transporters or their activity, which would be consistent with the postulated estrogen mediated down-regulation of PFOA transporters in rats (Kudo *et al.*, 2002). For the mouse and female rat the median fraction of blood flow to the filtrate (Q_{filc}) was physiologically relevant (less than or equal to the fraction of blood flow to the kidney) and the 95% credible intervals were within the range of the cardiac output. The estimated flow to the filtrate was more uncertain for the male rat and cynomolgus monkey: the medians were larger than physiologically plausible (Davies and Morris, 1993), 22% and 15% respectively, but the 95% credible intervals spanned three orders of magnitude.

2) PFOS PK parameters

The estimated PK parameters (median and 95% interval) for PFOS are presented in Table 7. Parameters for the male mouse were extremely uncertain, leading to relatively large credible intervals on predicted dose metrics. This uncertainty reflects a

combination of the limited amount of data (only two, single dose treatments – see Table 4) and perhaps the inappropriateness of the model used. For other species and genders the PFOS data were relatively more certain. The PK data for PFOS in male and female rats and monkeys were consistent with the saturable resorption interpretation of non-linear PK. The median male and female rat parameters were dissimilar, but the difference was not statistically significant. The median fraction of blood flow to the filtrate (Q_{filc}) was physiologically relevant for the male and female rats, but appeared too high for the mouse and monkeys.

Curran *et al.* (2008) reported a final serum concentration of PFOS in male and female rats four to eight times less than was predicted by the calibrated model. Since the PK model does well for other studies, this discrepancy appears to indicate a either a problem with our characterization of that study (e.g. assumptions about dose received from feed) or differences with the analytical chemistry method used.

Comparison of dose metrics

The full PK parameter distributions from the analysis of *in vivo* PK data were used to predict the 95% credible intervals for dose metrics corresponding to each LOEL and NOEL treatment group. Details for all predicted dose metrics corresponding to each LOEL are reported in Supplemental Table 7 and Supplemental Table 8

Figure 4 illustrates the consistency of predicted internal dose metrics corresponding to the LOEL for each *in vivo* study, given each study's respective treatment regimen. For each dose metric, *in vivo* endpoint, and chemical combination, the dose metrics for the various studies are scaled by the average value of the dose metric across those studies and the deviation from that average is plotted.

1) PFOA dose metrics

The mean and maximum serum concentrations appear to be the most consistent dose metrics in Figure 4, with most scaled values near zero (small deviation from perfect) despite the occasional outlier study. This is in agreement with Rodriguez *et al.* (2009) in which PFOA *in vivo* toxicological studies with similar toxicity endpoints in rats and mice differed by thirty-fold (3 mg/kg/day and 0.1 mg/kg/day, respectively) in administered dose. By investigating the PK for the two different LOELs, Rodriguez *et al.* (2009) determined that the time-integrated serum concentrations (AUC) values were in fact similar.

PFOA hepatic effects have the most *in vivo* studies shown in Figure 4. For this combination of chemical and effect, there are ten different *in vivo* LOELs from six studies (note that Wolf *et al.* (2007) identified five different LOELs for dosing on different windows of gestational days, e.g. days 7 through 17). For PFOA hepatic effects the outliers with respect to total dose and AUC are from the 180 day monkey study (Butenhoff *et al.*, 2002). Although that study had a LOEL of 3 mg/kg/day, which is superficially similar to the LOELs of the other studies, the total dose of 540 mg/kg is a clear outlier with respect to the other studies. The AUC for the 180 day study is also an outlier relative to the more acute studies. For both PFOA hepatic and developmental effects, the most consistent dose metrics are mean and maximum serum concentration.

2) PFOS dose metrics

For PFOS immunological effects, there are only three LOELs from two studies – Dong *et al.* (2009) studied male mice, while Peden-Adams *et al.* (2008) studied male and female mice. The Peden-Adams *et al.* (2008) study found LOELs of 0.0018 and 0.0036 mg/kg/day compared with the Dong *et al.* (2009) LOEL of 0.083 mg/kg/day and PK does not appear to explain the inconsistency. Similarly the Lau *et al.* (2003) PFOS developmental LOEL is 10 mg/kg/day, roughly ten times greater than the Butenhoff, *et al.* (2009), Thibodeaux *et al.* (2003) and Luebker *et al.* (2005b) dose metrics for developmental effects. No single dose metric appears to reconcile all the PFOS thyroid, reproductive, or liver effects.

Analysis of the Onset of *in vivo* effects

For each observed *in vivo* effect in Figures 5 and 6 the 95% credible interval of the predicted mean serum concentration dose metrics can be used to identify a transition region between the NOEL and LOEL groups. In this way we identify whether or not there is a mean serum concentration that corresponds to the onset of each effect that is consistent across studies (and therefore between species). If there is no NOEL dose group, all we know is that the effect happened somewhere between the mean concentration for no dose (zero) and the dose metric for the LOEL dose group. However we can assume that an arbitrary level of LOEL/100 there may be no activity detected. In Tables 8 and 9 the transition region of mean serum concentrations transition from NOEL to LOEL are organized by endpoint, using information across all species and studies to bracket a transition region in which PFOS or PFOA may have initiated toxic events.

1) Onset of PFOA Effects

Figure 5 compares the predicted mean serum concentration dose metric corresponding to the LOEL treatment group for each PFOA *in vivo* study. Where available, the dose metric for the NOEL treatment groups is also shown, but for most PFOA studies the lowest dose group had an effect (*i.e.*, the lowest dose group is the LOEL and there is no NOEL). Regardless of species or endpoint, the LOELs in Figure 5 appear to be roughly consistent. Although the lack of NOELs for most studies makes it hard to evaluate whether this is simply a consequence of dose spacing; the number of studies and varying kinetics between species and genders makes it unlikely that this consistency is entirely due to chance. In Table 8, the transitions from NOEL to LOEL for PFOA are organized by endpoint.

All three dose metrics (mean and maximum serum concentration and AUC) for each *in vivo* study are presented in Supplemental Table 7. These estimated internal doses are

1
2
3 slightly higher than Rodriguez *et al.* (2009), which found that 1 mg/kg/day in the Lau *et*
4 *al.* (2006) study result in an AUC of 9864 mg/L*hr (converted from an average daily
5 AUC of 548 mg/L*hr by multiplying by 18 days) compared to the estimate of 19600
6 (686) mg/L*hr reported here.
7
8
9

10
11
12 **2) Onset of PFOS Effects**
13
14

15
16 In Figure 6 the PFOS *in vivo* effects have been compared using the predicted mean
17 serum concentration dose metric across studies, species, and genders. Unlike with
18 PFOA, the presence of NOELs for most PFOS studies allows clear argument that the
19 dose metrics are generally consistent. The LOELs and NOELs for the three studies with
20 thyroid effects are entirely consistent, but for each of liver, developmental, reproductive,
21 and immunological effects there is one outlier study (e.g. a study with a NOEL predicted
22 higher than LOELs of the other studies). In Table 9 the window of concentrations for the
23 transition from NOEL to LOEL for PFOS are organized by endpoint, and due to the
24 outlier studies only thyroid effects have an intersection transition region (*i.e.* a transition
25 region that is consistent for all studies).
26
27
28
29
30
31
32
33

34
35 The LOELs and NOELs for liver effects are consistent for four studies, but the Curran,
36 *et al.* (2008) female rat LOEL is lower than the NOEL for the other four studies,
37 including the Curran, *et al.* (2008) male rat study. For developmental effects, the LOELs
38 and NOELs are consistent for four studies, but the Lau, *et al.* (2003) mouse study has a
39 NOEL higher than the LOELs of the other studies (which were all rat studies). For the
40 three studies showing reproductive effects, the Chen, *et al.* (2012) LOEL is higher than
41 the NOEL for the Luebker, *et al.* (2005a) study.
42
43
44
45
46
47
48

49 Immunological effects for PFOS appear to be much more sensitive than the other
50 endpoints observed. However, there is disagreement between the predicted dose
51 metrics for the Dong, *et al.* (2009) and the Peden-Adams, *et al.* (2008) studies since the
52 Peden-Adams, *et al.* (2008) study identified a LOEL of 0.00018 mg/kg/day for
53
54
55
56
57
58
59
60

1
2
3 suppressed sheep red blood cell plaque-forming cell response while the Dong, *et al.*
4 (2009) LOEL was 0.008 mg/kg/day for increased splenic natural killer cell activity.
5
6
7

8
9 All three dose metrics (mean and maximum serum concentration and AUC) for each
10 PFOS *in vivo* study are presented in Supplemental Table 8.
11
12

13 14 **Comparison with *in vitro* Data**

15
16
17 The 95% credible interval of the dose metrics for the LOEL and NOEL (or LOEL/100)
18 demarked a transition region within which biological perturbations sufficient to produce a
19 phenotypic toxic response may be presumed to occur (Tables 8 and 9). If the AC₅₀ for
20 an *in vitro* assay lies within a NOEL-LOEL transition region, then the bioactivity
21 characterized by that assay occurs at a concentration higher than that of the lowest
22 NOEL dose group, and lower than those of the highest LOEL group.
23
24
25
26
27
28

29
30 The coincidence of specific assays with specific effects is summarized in Tables 10 and
31 11, where a “weak” coincidence is an overlap between one or more NOEL-LOEL
32 transition regions for a specific endpoint, and a “strong” coincidence is an overlap with
33 the NOEL-LOEL transition regions for all studies for a specific endpoint.
34
35
36
37

38
39 Tables 10 and 11 contain a column indicating whether or not an assay was active for
40 both PFOS and PFOA. There are three such assays, which are described in Table 5.
41 Of them, only the NVS_ENZ_hTie2 assay can be easily correlated with a toxic effect, as
42 Tie2 is associated with angiogenesis, a key process in development, and therefore
43 potentially a mechanism for PFC-induced developmental toxicity (Kleinstreuer, *et al.*,
44 2011). Both PFCs activate the NVS_ENZ_hBACE assay, and BACE is associated with
45 Alzheimer’s disease (Vassar *et al.*, 2009), but this is not an endpoint that can be
46 explored with the type of animal studies analyzed here. The activation of PXRE
47 indicated by the ATG_PXRE_CIS assay for both chemicals is most likely an indicator of
48 xenobiotic sensing only, since PFCs are not metabolized.
49
50
51
52
53
54
55
56
57
58
59
60

Also summarized in Tables 10 and 11 is whether or not the given assay is an element of a published *in vitro* signature for toxicity. In Martin, *et al.* (2011) several *in vitro* assays were identified as being correlated with reproductive toxicity in rats (*i.e.* an *in vitro* “signature” for rat reproductive toxicity). In Sipes, *et al.* (2011) separate *in vitro* signatures were developed for rat and rabbit developmental toxicity. Finally, in Kleinstreuer, *et al.* (2011) and Knudsen and Kleinstreuer (2011) an *in vitro* signature for vascular disrupters has been developed

1) PFOA in vitro data

Twelve *in vitro* activities are listed for PFOA in Table 10, and the corresponding concentrations are also plotted as horizontal lines in Figure 5. The lack of NOELs for many of the PFOA studies produces broad transition regions: all assays that are below the LOELs for developmental and immunological endpoints appear consistent with those effects (*i.e.*, they activate at concentrations greater than the highest LOEL/100). Three assays are consistent with all NOELs and LOELs for the PFOA assays: NVS_ENZ_hTie2, ATG_PPARGa_TRANS_perc, and ATG_PPARGa_CIS_perc. Where benchmark doses could be calculated, they coincide with the onset of *in vitro* activity.

As shown in Table 10, five of the twelve PFOA-activated assays are part of the Martin, *et al.* (2011) signature for rat reproductive toxicity. Only one of the active *in vitro* assays for PFOA is in the Sipes, *et al.* (2011) rat developmental toxicity signature and none are in the signature for rabbit developmental toxicity. Four PFOA *in vitro* activities are consistent with the Kleinstreuer, *et al.* (2011) vascular disruption signature. The cell-free ENZ_hTie2 assay from NovaScreen, which was also active for PFOS, activated in the transition region for all observed effects and was also present in the vascular disrupter toxicity signature.

2) PFOS in vitro data

The AC₅₀s for the PFOS *in vitro* assays plotted in Figure 6 also seem to be generally consistent with the onset of potentially toxic endpoints. There were 52 assays in which activity was observed, of which only those assays active in one of the toxicity signatures or also found for PFOA are listed in Table 11. The full list of active assays for PFOS is available in Supplemental Table 9.

Due to the different NOEL-LOEL transition regions for immunological effects and all other effects, the assays were divided into two different sets coincident with the transition regions. The 18 most potent assays are coincident with the immunological effects transition from LOEL to NOEL, and some of these assays are also found in the rat reproductive toxicity signature from Martin, *et al.* (2011).

Many other PFOS-activated *in vitro* assays (n=40) are strongly coincident with the thyroid effects. Due to outlier *in vivo* toxicity studies, assays are only weakly consistent with the remaining effects. Six active assays are associated with the Martin, *et al.* (2011) rat reproductive toxicity signature. Four active assays are associated with the Knudsen and Kleinstreuer (2011) vascular disrupter signature.

DISCUSSION

This study provides dosimetry for twenty-two different toxicological *in vivo* studies across species, strains, and genders and compares predicted serum concentrations with *in vitro* concentrations necessary for activity in high-throughput assays. For a given effect we found that the predicted dose metrics corresponding to the onset of that effect were generally consistent across gender and species, despite well known differences in the PK. This consistency between studies suggests that rather than a singular, “most sensitive” test animal and effect, that there were multiple potential adverse effects occurring across species for a variety of dose regimens that produced mean serum concentrations of approximately 50 µM for both PFOA and PFOS.

We also found that the concentrations that cause *in vitro* bioactivity from some ToxCast assays appear to be consistent with the predicted serum concentrations for the transition from NOEL to LOEL dose regimens. For both PFOS and PFOA, it appears that the onset of *in vivo* effects occurs for dose regimens that produce average concentrations in excess of concentrations needed to cause bioactivity *in vitro*. For the PFOS studies, which had several observed groups with no observed effect, the NOEL dose regimens produced concentrations too low to cause much bioactivity *in vitro*. Most of the PFOS *in vitro* activity occurs in a cluster between 11.6 and 30.1 μM – a relatively narrow band of concentrations which are consistent with transition from NOEL to LOEL for all of the thyroid *in vivo* toxicity studies and most of the liver, developmental and reproductive studies.

For PFOA there are two clusters of activity among the PFOA *in vitro* data at ~ 5 μM and ~ 50 μM . Despite nine PFOA *in vivo* studies, there were few NOEL dose groups, so it is hard to say which cluster predicts the onset of effects, although ~ 50 μM is consistent with the BMD from the Wolf *et al.* (2007) study. For all but the DeWitt *et al.* (2008) liver effects, both clusters provide a conservative estimate of the needed serum concentration for observed effect, and the second cluster is within the 95% credible interval for the DeWitt *et al.* (2008) study. For both PFOA and PFOS a conservative estimate of the dose regimens needed to produce non-specific (*i.e.*, hepatic, thyroid, developmental, or reproductive) toxicity *in vivo* could have been predicted from *in vitro* bioactivity given sufficient PK data.

In order to facilitate dosimetric anchoring, we used a Bayesian framework to incorporate uneven amounts of PK data from eight *in vivo* studies that used varying animals and dosing regimens. Model parameter distributions for a consistent PK model were estimated such that a 95% credible interval for each dose metric could be predicted. The breadth of the credible interval of the predicted dose metrics reflects the uncertainty corresponding to the appropriateness of the PK model used and the available *in vivo* PK data sets for each species, strain/stock, and gender.

1
2
3 The mean and maximum serum concentrations were both identified as being generally
4 consistent dosimetric anchors. Choosing between them depends on understanding the
5 mechanism of action: perhaps maximum serum concentration for acute effects as
6 opposed to mean serum concentration for chronic effects.
7
8
9

10
11 PFOA is known to have dose-dependent (non-linear) pharmacokinetic properties:
12 though repeated doses rapidly accumulate to a quasi-equilibrium blood concentration, a
13 single dose results in a much longer half-life than would be consistent with the rapid
14 approach to quasi-equilibrium (Andersen, *et al.*, 2006; Lou, *et al.*, 2009). Given its long
15 half-life, using a linear PK model (e.g. the one-compartment model) to predict
16 exposures resulting from multiple PFOA exposures results in large overestimates of
17 reality (Butenhoff, *et al.*, 2004b; Lou, *et al.*, 2009). The empirical saturable renal
18 resorption model (Andersen, *et al.*, 2006) addresses this problem by allowing PFOA to
19 reach steady state faster than the elimination half-life would indicate. Because it is an
20 empirical model, species-specific parameters must be estimated using species-specific
21 PK data.
22
23
24
25
26
27
28
29
30
31

32
33 A physiologically-based PK (PBPK) model for PFCs might be preferable because it
34 would allow extrapolation between species, provide better estimates of chemical-
35 specific parameters, and allow estimation of chemical concentration in the specific
36 tissues for which toxicity is observed. However, data for chemical-specific partitioning
37 into most tissues exists only for PFOA, and then only from the single-dose Kemper
38 (2003) rat study. We have found here that due to the dose selection of the Kemper
39 (2003) study, the non-linear PK of PFOA was not present. This is indicated by the very
40 uncertain estimates of the Michaelis-Menten parameters for that study (Table 6). If the
41 non-linear PK for PFCs is due to tissue partitioning (e.g. binding or transport) then these
42 processes would be missed by the Kemper (2003) data set. The serum, urine, and
43 feces data from Kemper (2003) was found to be well fit by a linear, two-compartment
44 model using a single distribution of parameters for all doses in Wambaugh *et al.* (2008).
45 A more physiologically-motivated PK model for PFOA in humans exists (Loccisano *et*
46 *al.*, 2011) but, as with the Andersen, *et al.* (2006) model, the elimination parameters
47
48
49
50
51
52
53
54
55
56
57
58
59
60

cannot be extrapolated and must be empirically determined. Given the limitations of the available data for estimating parameters, the simpler Andersen, *et al.* (2006) empirical PK model was preferable.

The general concordance observed in Table 6 and Table 7 of the saturable resorption parameter estimates with kidney blood flow/glomerular filtration rates provides support for the renal resorption interpretation of the Andersen *et al.* (2006) model. However, until a PK study with matched tissue and urine samples is conducted at doses resulting in non-linear PK, the saturable resorption mechanism remains one plausible hypothesis among many (e.g. sequestration in the liver, saturation of plasma protein binding), particularly because organic anion transporters are expressed in many tissues beyond the kidney proximal tubule.

Across the nine *in vivo* studies for PFOA the most sensitive toxic endpoint with respect to maximum and mean predicted serum concentration (all dose metrics given in Supplemental Tables 7 and 8) was for female C57BL/6N mice exposed to 0.94 mg/kg daily for fifteen days via drinking water (average daily water consumption was used). In this study increased absolute and relative liver weight was observed (DeWitt, *et al.*, 2008). The nine PFOA *in vivo* toxicity studies often lacked NOEL dose groups, indicating a need for lower doses in any future PFOA study designs.

Across the thirteen *in vivo* studies for PFOS, immunological effects appear to occur at lower doses than other effects. The three lowest exposures corresponding to endpoints were all for CD1 mice, indicating that CD1 mouse is the most sensitive animal among those tested. The available PFOS PK data were minimal for these animals, so the dosimetry is more uncertain. However, the range of possible internal doses indicated by the Bayesian analysis does not overlap with other studies.

When we move beyond the *in vivo* toxicity studies to compare with the *in vitro* assays we again observe some consistency. For PFOA the cell-free human TIE2 (ENZ_hTie2) assay from NovaScreen activated in the transition region for all observed effects and

was also active for non-immunological PFOS effects. TIE2 is associated with angiogenesis, a key process in development, and therefore potentially a mechanism for PFC-induced developmental toxicity (Kleinstreuer, *et al.*, 2011). For PFOS the *in vitro* assays coincident with *in vivo* immunological effects included inhibition of multiple metabolizing enzyme (CYP 450) activities. This indicates that there is plausible PFOS biological activity at these relatively low concentrations (the most potent activity was 0.066 μM). However, we are unaware of a linkage between the inhibition of CYP 450 and immunological endpoints. In three cases of missing NOEL groups for PFOA, sufficient data were available to estimate BMDs. Although a BMD does not allow analysis of which *in vitro* assays activated between the NOEL and LOEL groups, in two of the cases the BMD was consistent with the onset of *in vitro* activity.

The diversity of molecular targets affected by either PFOS or PFOA across ToxCast is broad and includes many not previously associated with PFCs. The ToxCast *in vitro* assays are primarily screening assays; the concentrations tested are broadly spaced (typically eight concentrations at half-log spacing from 100 μM to 0.01 μM) and the off-the-shelf assays do not necessarily investigate the most relevant key events for PFCs. Therefore these assays are not conclusive with respect to linking chemical effect to molecular target, *e.g.* more definitive follow-up work would be required. However, because the range of AC_{50}s across the targets lie in relatively narrow bands, an analysis based on these promiscuous activities may still be useful in defining the concentrations at which these chemicals interact with biological targets. Similar concordance between the serum levels demarking the transition from no effect to toxicity endpoint have been observed by Aylward and Hays (2011) for five ToxCast chemicals, including PFOA.

It remains to be seen whether, given sufficient PK knowledge, *in vitro* assays for other chemicals will correspond to *in vivo* effects. The lack of metabolism of PFCs makes comparison between *in vitro* bioactivity and the onset of endpoints in the *in vivo* toxicity studies more direct; however, there are still confounders of *in vitro-in vivo* extrapolation to be considered. Foremost is the fact that PFOA and PFOS bind well to serum albumin, leaving relatively little free compound to perturb biological activity (other than

displacing other albumin substrates). Due to differences in the concentration of serum albumin present in the *in vitro* assays (the cell-free assays had none) and the concentration of serum albumin present *in vivo*, the concentrations necessary to produce the same free fraction of PFCs may have varied by as much as two orders of magnitude (Gulden and Seibert, 2003).

Further, the frank concentration applied to the well may not reflect the concentration at the site of action. For both cell-free and cell-based *in vitro* assays the partitioning of compound between the wall of the well and proteins and lipids within the media, as well as the concentration within the cells themselves for cell-based assays are generally unknown (Zaldívar Comenges *et al.*, 2012). Though approaches exist for estimating well partitioning and media binding for many classes of organic compounds, these properties need to be investigated for PFCs.

Finally, most ToxCast assays are conducted in a concentration-response format and, if the response can be successfully fit with a Hill function, the concentration producing 50% maximal response activity (AC_{50}) was determined. In terms of toxicity, there is nothing necessarily unique about 50% activity; the AC_{50} merely provides a reasonable representation of the potency of a chemical for a given target. A Hill fit with a typical biological slope of one, has a range covering almost two orders of magnitude between the AC_{10} and the AC_{90} .

The observed coincidence between *in vitro* and *in vivo* concentrations indicates that these considerations may not be necessarily present or are offsetting in the case of PFOA and PFOS. However, the wide Phase I ToxCast concentration ranges are not optimal for testing these hypotheses. Therefore, these results should be used to prioritize resources for targeted testing of PFOA and PFOS, *e.g.* with a range of test concentrations that is denser than the half-log concentration spacing used for ToxCast screening.

Dosimetric anchoring via PK modeling demonstrated consistency between *in vivo* studies, nine for PFOA and thirteen for PFOS. Further, *in vitro* bioactivity data were consistent with *in vivo* dose-response, suggesting that for these compounds an estimate of the dose regimens needed to produce *in vivo* toxicity could have been predicted *in vitro*. Hogue (2012) indicates that there is a strong movement among international government bodies to phase out or ban long-chain PFCs in preference for shorter-chain PFCs worldwide. However, there is lack of toxicity information to address the potential adverse human health effects and environmental impacts of the shorter-chain PFCs. Therefore it would useful to provide predicted toxicity dose regimens for the shorter-chain PFCs as they are considered for replacement of the long-chain PFCs. Given the current state of knowledge despite twenty-two *in vivo* toxicity studies, e.g. many effects lacking NOELs, *in vitro* methods may provide a viable supplemental tool for hazard assessment.

ACKNOWLEDGEMENTS

The United States Environmental Protection Agency through its Office of Research and Development funded and managed the research described here. We thank Chester Rodriguez, Kevin Crofton, Paul Schlosser, and Susan Hester of the EPA for comments.

DISCLAIMER

The views expressed in this paper are those of the authors and do not necessarily reflect the views or policies of the U.S. Environmental Protection Agency.

References

(2010). *ToxCast Phase I and II Chemicals*. Available at:
<http://www.epa.gov/ncct/toxcast/files/ToxCast%20Chemical%20Summary%2014Dec2010.pdf>.
Accessed 1/26 2012.

Allen, B. C., Kavlock, R. J., Kimmel, C. A. and Faustman, E. M. (1994). Dose—Response Assessment for Developmental Toxicity: II. Comparison of Generic Benchmark Dose Estimates with No Observed Adverse Effect Levels. *Toxicological Sciences* **23**(4), 487-495, 10.1093/toxsci/23.4.487.

Andersen, M. E., Clewell, H. J., Tan, Y.-M., Butenhoff, J. L. and Olsen, G. W. (2006). Pharmacokinetic modeling of saturable, renal resorption of perfluoroalkylacids in monkeys--probing the determinants of long plasma half-lives. *Toxicology* **227**(16978759), 156-164.

Aylward, L. L. and Hays, S. M. (2011). Consideration of dosimetry in evaluation of ToxCast™ data. *Journal of Applied Toxicology* **31**(8), 741-751, 10.1002/jat.1626.

Bartell, S. M., Calafat, A. M., Lyu, C., Kato, K., Ryan, P. B. and Steenland, K. (2010). Rate of decline in serum PFOA concentrations after granular activated carbon filtration at two public water systems in Ohio and West Virginia. *Environ Health Perspect* **118**(20123620), 222-228.

Best, N., Cowles, M. and Vines, K. (1995). CODA: convergence diagnosis and output analysis for Gibbs sampling output.

Bjornsson, T. D., Callaghan, J. T., Einolf, H. J., Fischer, V., Gan, L., Grimm, S., Kao, J., King, S. P., Miwa, G., Ni, L., Kumar, G., McLeod, J., Obach, S. R., Roberts, S., Roe, A., Shah, A., Snikeris, F., Sullivan, J. T., Tweedie, D., Vega, J. M., Walsh, J. and Wrighton, S. A. (2003). The Conduct of In Vitro and In Vivo Drug-Drug Interaction Studies: A PhRMA Perspective. *The Journal of Clinical Pharmacology* **43**(5), 443-469, 10.1177/0091270003252519.

Blaauboer, B. J. (2010). Biokinetic Modeling and in Vitro–in Vivo Extrapolations. *Journal of Toxicology and Environmental Health, Part B* **13**(2-4), 242-252, 10.1080/10937404.2010.483940.

Boobis, A. R. (2010). Mode of Action Considerations in the Quantitative Assessment of Tumour Responses in the Liver. *Basic & Clinical Pharmacology & Toxicology* **106**(3), 173-179, 10.1111/j.1742-7843.2009.00505.x.

Butenhoff, J., Costa, G., Elcombe, C., Farrar, D., Hansen, K., Iwai, H., Jung, R., Kennedy, G., Lieder, P., Olsen, G. and Thomford, P. (2002). Toxicity of ammonium perfluorooctanoate in male cynomolgus monkeys after oral dosing for 6 months. *Toxicological sciences : an official journal of the Society of Toxicology* **69**(12215680), 244-257.

Butenhoff, J. L., Kennedy, G. L., Frame, S. R., O'Connor, J. C. and York, R. G. (2004a). The reproductive toxicology of ammonium perfluorooctanoate (APFO) in the rat. *Toxicology* **196**(15036760), 95-9116.

Butenhoff, J. L., Kennedy, G. L., Hinderliter, P. M., Lieder, P. H., Jung, R., Hansen, K. J., Gorman, G. S., Noker, P. E. and Thomford, P. J. (2004b). Pharmacokinetics of Perfluorooctanoate in Cynomolgus Monkeys. *Toxicological Sciences* **82**(2), 394-406, 10.1093/toxsci/kfh302.

Butenhoff, J. L., Ehresman, D. J., Chang, S.-C., Parker, G. A. and Stump, D. G. (2009). Gestational and lactational exposure to potassium perfluorooctanesulfonate (K+PFOS) in rats: Developmental neurotoxicity. *Reproductive Toxicology* **27**(3–4), 319-330, 10.1016/j.reprotox.2008.12.010.

- Calafat, A. M., Kuklenyik, Z., Reidy, J. A., Caudill, S. P., Tully, J. S. and Needham, L. L. (2007). Serum Concentrations of 11 Polyfluoroalkyl Compounds in the U.S. Population: Data from the National Health and Nutrition Examination Survey (NHANES) 1999–2000. *Environmental Science & Technology* **41**(7), 2237–2242, 10.1021/es062686m.
- Chang, S.-C., Thibodeaux, J. R., Eastvold, M. L., Ehresman, D. J., Bjork, J. A., Froehlich, J. W., Lau, C., Singh, R. J., Wallace, K. B. and Butenhoff, J. L. (2008). Thyroid hormone status and pituitary function in adult rats given oral doses of perfluorooctanesulfonate (PFOS). *Toxicology* **243**(18063289), 330–339.
- Chang, S.-C., Ehresman, D. J., Bjork, J. A., Wallace, K. B., Parker, G. A., Stump, D. G. and Butenhoff, J. L. (2009). Gestational and lactational exposure to potassium perfluorooctanesulfonate (K+PFOS) in rats: toxicokinetics, thyroid hormone status, and related gene expression. *Reprod Toxicol* **27**(19429409), 387–399.
- Chang, S.-C., Noker, P. E., Gorman, G. S., Gibson, S. J., Hart, J. A., Ehresman, D. J. and Butenhoff, J. L. (2012). Comparative pharmacokinetics of perfluorooctanesulfonate (PFOS) in rats, mice, and monkeys. *Reproductive Toxicology* **33**(4), 428–440, 10.1016/j.reprotox.2011.07.002.
- Chen, T., Zhang, L., Yue, J.-q., Lv, Z.-q., Xia, W., Wan, Y.-j., Li, Y.-y. and Xu, S.-q. (2012). Prenatal PFOS exposure induces oxidative stress and apoptosis in the lung of rat off-spring. *Reproductive Toxicology* **33**(4), 538–545, 10.1016/j.reprotox.2011.03.003.
- Curran, I., Hierlihy, S. L., Liston, V., Pantazopoulos, P., Nunnikhoven, A., Tittlemier, S., Barker, M., Trick, K. and Bondy, G. (2008). Altered Fatty Acid Homeostasis and Related Toxicologic Sequelae in Rats Exposed to Dietary Potassium Perfluorooctanesulfonate (PFOS). *Journal of Toxicology and Environmental Health, Part A* **71**(23), 1526–1541, 10.1080/15287390802361763.
- Davies, B. and Morris, T. (1993). Physiological Parameters in Laboratory Animals and Humans. *Pharmaceutical Research* **10**(7), 1093–1095, 10.1023/a:1018943613122.
- DeWitt, J. C., Copeland, C. B., Strynar, M. J. and Luebke, R. W. (2008). Perfluorooctanoic acid-induced immunomodulation in adult C57BL/6J or C57BL/6N female mice. *Environ Health Perspect* **116**(18470313), 644–650.
- Dong, G.-H., Zhang, Y.-H., Zheng, L., Liu, W., Jin, Y.-H. and He, Q.-C. (2009). Chronic effects of perfluorooctanesulfonate exposure on immunotoxicity in adult male C57BL/6 mice. *Arch Toxicol* **83**(19343326), 805–815.
- Garcia, R. I., Wambaugh, J. F., Kenyon, E. M., Ibrahim, J. G. and Setzer, R. W. (2013). Identifiability of PBPK Models with Applications to Dimethylarsinic Exposure, *in preparation*.
- Gelman, A., Carlin, J., Stern, H. and Rubin, D. (2004). *Bayesian data analysis*. 2nd ed. Chapman and Hall/CRC.
- Harada, K. H., Yang, H. R., Moon, C. S., Hung, N. N., Hitomi, T., Inoue, K., Niisoe, T., Watanabe, T., Kamiyama, S., Takenaka, K., Kim, M. Y., Watanabe, K., Takasuga, T. and Koizumi, A. (2010). Levels of perfluorooctane sulfonate and perfluorooctanoic acid in female serum samples from Japan in 2008, Korea in 1994–2008 and Vietnam in 2007–2008. *Chemosphere* **79**(3), 314–319.
- Hastings, W. K. (1970). Monte Carlo sampling methods using Markov chains and their applications. *Biometrika* **57**(1), 97–109, 10.1093/biomet/57.1.97.
- Haug, L. S., Thomsen, C. and Becher, G. (2009). Time Trends and the Influence of Age and Gender on Serum Concentrations of Perfluorinated Compounds in Archived Human Samples. *Environmental Science & Technology* **43**(6), 2131–2136, 10.1021/es802827u.

- Heidelberger, P. and Welch, P. (1983). Simulation run length control in the presence of an initial transient. *Operations Research* **31**, 1109-44.
- Hogue, C. (2012). Perfluorinated Chemical Controls. In *Chemical & Engineering News* (pp. 24-25).
- Houck, K. A., Dix, D. J., Judson, R. S., Kavlock, R. J., Yang, J. and Berg, E. L. (2009). Profiling Bioactivity of the ToxCast Chemical Library Using BioMAP Primary Human Cell Systems. *Journal of Biomolecular Screening* **14**(9), 1054-1066, 10.1177/1087057109345525.
- Judson, R. S., Houck, K. A., Kavlock, R. J., Knudsen, T. B., Martin, M. T., Mortensen, H. M., Reif, D. M., Rotroff, D. M., Shah, I., Richard, A. M. and Dix, D. J. (2009). In Vitro Screening of Environmental Chemicals for Targeted Testing Prioritization: The ToxCast Project. *Environmental Health Perspectives* **118**(4).
- Judson, R. S., Houck, K. A., Kavlock, R. J., Knudsen, T. B., Martin, M. T., Mortensen, H. M., Reif, D. M., Rotroff, D. M., Shah, I., Richard, A. M. and Dix, D. (2010). In Vitro Screening of Environmental Chemicals for Targeted Testing Prioritization: The ToxCast Project. *Environmental Health Perspectives* **118**(4), 485-492, 10.1289/ehp.0901392.
- Judson, R. S., Kavlock, R. J., Setzer, R. W., Cohen-Hubal, E. A., Martin, M. T., Knudsen, T. B., Houck, K. A., Thomas, R. S., Wetmore, B. A. and Dix, D. J. (2011). Estimating Toxicity-Related Biological Pathway Altering Doses for High-Throughput Chemical Risk Assessment. *Chemical Research in Toxicology* **24**(4), 451-462, 10.1021/tx100428e.
- Kemper, R. (2003). Perfluorooctanoic acid: toxicokinetics in the rat. USEPA Administrative Record AR-226.1499.
- Kleinstreuer, N. C., Judson, R. S., Reif, D. M., Sipes, N. S., Singh, A. V., Chandler, K. J., DeWoskin, R., Dix, D. J., Kavlock, R. J. and Knudsen, T. B. (2011). Environmental Impact on Vascular Development Predicted by High-Throughput Screening. *Environ Health Perspect* **119**(11).
- Knudsen, T. B., Houck, K. A., Sipes, N. S., Singh, A. V., Judson, R. S., Martin, M. T., Weissman, A., Kleinstreuer, N. C., Mortensen, H. M., Reif, D. M., Rabinowitz, J. R., Setzer, R. W., Richard, A. M., Dix, D. J. and Kavlock, R. J. (2011). Activity profiles of 309 ToxCast™ chemicals evaluated across 292 biochemical targets. *Toxicology* **282**(1-2), 1-15, 10.1016/j.tox.2010.12.010.
- Knudsen, T. B. and Kleinstreuer, N. C. (2011). Disruption of embryonic vascular development in predictive toxicology. *Birth Defects Research Part C: Embryo Today: Reviews* **93**(4), 312-323, 10.1002/bdrc.20223.
- Kudo, N., Katakura, M., Sato, Y. and Kawashima, Y. (2002). Sex hormone-regulated renal transport of perfluorooctanoic acid. *Chem Biol Interact* **139**(11879818), 301-316.
- Lau, C., Thibodeaux, J. R., Hanson, R. G., Rogers, J. M., Grey, B. E., Stanton, M. E., Butenhoff, J. L. and Stevenson, L. A. (2003). Exposure to perfluorooctane sulfonate during pregnancy in rat and mouse. II: postnatal evaluation. *Toxicological sciences : an official journal of the Society of Toxicology* **74**(12773772), 382-392.
- Lau, C., Butenhoff, J. L. and Rogers, J. M. (2004). The developmental toxicity of perfluoroalkyl acids and their derivatives. *Toxicology and Applied Pharmacology* **198**(2), 231-241, <http://dx.doi.org/10.1016/j.taap.2003.11.031>.
- Lau, C., Thibodeaux, J. R., Hanson, R. G., Narotsky, M. G., Rogers, J. M., Lindstrom, A. B. and Strynar, M. J. (2006). Effects of perfluorooctanoic acid exposure during pregnancy in the mouse. *Toxicological sciences : an official journal of the Society of Toxicology* **90**(16415327), 510-518.

- Lau, C., Anitole, K., Hodes, C., Lai, D., Pfahles-Hutchens, A. and Seed, J. (2007). Perfluoroalkyl acids: a review of monitoring and toxicological findings. *Toxicological sciences : an official journal of the Society of Toxicology* **99**(17519394), 366-394.
- Loccisano, A. E., Campbell Jr, J. L., Andersen, M. E. and Clewell Iii, H. J. (2011). Evaluation and prediction of pharmacokinetics of PFOA and PFOS in the monkey and human using a PBPK model. *Regulatory Toxicology and Pharmacology* **59**(1), 157-175, <http://dx.doi.org/10.1016/j.yrtph.2010.12.004>.
- Lou, I., Wambaugh, J. F., Lau, C., Hanson, R. G., Lindstrom, A. B., Strynar, M. J., Zehr, R. D., Setzer, R. W. and Barton, H. A. (2009). Modeling single and repeated dose pharmacokinetics of PFOA in mice. *Toxicological sciences : an official journal of the Society of Toxicology* **107**(19005225), 331-341.
- Luebker, D. J., Case, M. T., York, R. G., Moore, J. A., Hansen, K. J. and Butenhoff, J. L. (2005a). Two-generation reproduction and cross-foster studies of perfluorooctanesulfonate (PFOS) in rats. *Toxicology* **215**(16146667), 126-148.
- Luebker, D. J., York, R. G., Hansen, K. J., Moore, J. A. and Butenhoff, J. L. (2005b). Neonatal mortality from in utero exposure to perfluorooctanesulfonate (PFOS) in Sprague-Dawley rats: Dose-response, and biochemical and pharmacokinetic parameters. *Toxicology* **215**(1-2), 149-169, [10.1016/j.tox.2005.07.019](http://dx.doi.org/10.1016/j.tox.2005.07.019).
- Martin, M. T., Judson, R. S., Reif, D. M., Kavlock, R. J. and Dix, D. J. (2009). Profiling Chemicals Based on Chronic Toxicity Results from the U.S. EPA ToxRef Database. *Environ Health Perspect* **117**(3), 392-399, [10.1289/ehp.0800074](http://dx.doi.org/10.1289/ehp.0800074).
- Martin, M. T., Dix, D. J., Judson, R. S., Kavlock, R. J., Reif, D. M., Richard, A. M., Rotroff, D. M., Romanov, S., Medvedev, A., Poltoratskaya, N., Gambarian, M., Moeser, M., Makarov, S. S. and Houck, K. A. (2010). Impact of Environmental Chemicals on Key Transcription Regulators and Correlation to Toxicity End Points within EPA's ToxCast Program. *Chemical Research in Toxicology* **23**(3), 578-590, [10.1021/tx900325g](http://dx.doi.org/10.1021/tx900325g).
- Martin, M. T., Knudsen, T. B., Reif, D. M., Houck, K. A., Judson, R. S., Kavlock, R. J. and Dix, D. J. (2011). Predictive Model of Rat Reproductive Toxicity from ToxCast High Throughput Screening. *Biology of Reproduction* **85**(2), 327-339, [10.1095/biolreprod.111.090977](http://dx.doi.org/10.1095/biolreprod.111.090977).
- Metropolis, N., Rosenbluth, A. W., Rosenbluth, M. N., Teller, A. H. and Teller, E. (1953). Equation of State Calculations by Fast Computing Machines. *The Journal of Chemical Physics* **21**(6), 1087-1092.
- Olsen, G. W., Burris, J. M., Ehresman, D. J., Froehlich, J. W., Seacat, A. M., Butenhoff, J. L. and Zobel, L. R. (2007). Half-life of serum elimination of perfluorooctanesulfonate, perfluorohexanesulfonate, and perfluorooctanoate in retired fluorochemical production workers. *Environ Health Perspect* **115**(17805419), 1298-1305.
- Olsen, G. W., Lange, C. C., Ellefson, M. E., Mair, D. C., Church, T. R., Goldberg, C. L., Herron, R. M., Medhdizadehkashi, Z., Nobiletti, J. B., Rios, J. A., Reagen, W. K. and Zobel, L. R. (2012). Temporal Trends of Perfluoroalkyl Concentrations in American Red Cross Adult Blood Donors, 2000-2010. *Environmental Science & Technology* **46**(11), 6330-6338, [10.1021/es300604p](http://dx.doi.org/10.1021/es300604p).
- Peden-Adams, M. M., Keller, J. M., Eudaly, J. G., Berger, J., Gilkeson, G. S. and Keil, D. E. (2008). Suppression of humoral immunity in mice following exposure to perfluorooctane sulfonate. *Toxicological sciences : an official journal of the Society of Toxicology* **104**(18359764), 144-154.

- Perkins, R. G., Butenhoff, J. L., Kennedy, G. L. and Palazzolo, M. J. (2004). 13-week dietary toxicity study of ammonium perfluorooctanoate (APFO) in male rats. *Drug Chem Toxicol* **27**(15573472), 361-378.
- R Development Core Team. (2012). *R: A Language and Environment for Statistical Computing*, Version 2.10.0 R Foundation for Statistical Computing, Vienna, Austria.
- Reif, D. M., Martin, M. T., Tan, S. W., Houck, K. A., Judson, R. S., Richard, A. M., Knudsen, T. B., Dix, D. J. and Kavlock, R. J. (2010). Endocrine Profiling and Prioritization of Environmental Chemicals Using ToxCast Data. *Environ Health Perspect* **118**(12).
- Rodriguez, C. E., Setzer, R. W. and Barton, H. A. (2009). Pharmacokinetic modeling of perfluorooctanoic acid during gestation and lactation in the mouse. *Reprod Toxicol* **27**(19429408), 373-386.
- Seacat, A. M., Thomford, P. J., Hansen, K. J., Olsen, G. W., Case, M. T. and Butenhoff, J. L. (2002). Subchronic toxicity studies on perfluorooctanesulfonate potassium salt in cynomolgus monkeys. *Toxicological sciences : an official journal of the Society of Toxicology* **68**(12075127), 249-264.
- Seacat, A. M., Thomford, P. J., Hansen, K. J., Clemen, L. A., Eldridge, S. R., Elcombe, C. R. and Butenhoff, J. L. (2003). Sub-chronic dietary toxicity of potassium perfluorooctanesulfonate in rats. *Toxicology* **183**(1-3), 117-131, 10.1016/s0300-483x(02)00511-5.
- Sipes, N. S., Martin, M. T., Reif, D. M., Kleinstreuer, N. C., Judson, R. S., Singh, A. V., Chandler, K. J., Dix, D. J., Kavlock, R. J. and Knudsen, T. B. (2011). Predictive Models of Prenatal Developmental Toxicity from ToxCast High-Throughput Screening Data. *Toxicological Sciences* **124**(1), 109-127, 10.1093/toxsci/kfr220.
- Soetaert, K., Petzoldt, T. and Setzer, R. W. (2010). Solving Differential Equations in R: Package deSolve. *Journal of Statistical Software* **33**(9), 1-25.
- Thibodeaux, J. R., Hanson, R. G., Rogers, J. M., Grey, B. E., Barbee, B. D., Richards, J. H., Butenhoff, J. L., Stevenson, L. A. and Lau, C. (2003). Exposure to perfluorooctane sulfonate during pregnancy in rat and mouse. I: maternal and prenatal evaluations. *Toxicological sciences : an official journal of the Society of Toxicology* **74**(12773773), 369-381.
- Vassar, R., Kovacs, D. M., Yan, R. and Wong, P. C. (2009). The β -Secretase Enzyme BACE in Health and Alzheimer's Disease: Regulation, Cell Biology, Function, and Therapeutic Potential. *The Journal of Neuroscience* **29**(41), 12787-12794, 10.1523/jneurosci.3657-09.2009.
- Wambaugh, J. F., Barton, H. A. and Setzer, R. W. (2008). Comparing models for perfluorooctanoic acid pharmacokinetics using Bayesian analysis. *J Pharmacokinet Pharmacodyn* **35**(19130186), 683-712.
- White, S. S., Kato, K., Jia, L. T., Basden, B. J., Calafat, A. M., Hines, E. P., Stanko, J. P., Wolf, C. J., Abbott, B. D. and Fenton, S. E. (2009). Effects of perfluorooctanoic acid on mouse mammary gland development and differentiation resulting from cross-foster and restricted gestational exposures. *Reprod Toxicol* **27**(19095057), 289-298.
- Wolf, C. J., Fenton, S. E., Schmid, J. E., Calafat, A. M., Kuklenyik, Z., Bryant, X. A., Thibodeaux, J., Das, K. P., White, S. S., Lau, C. S. and Abbott, B. D. (2007). Developmental toxicity of perfluorooctanoic acid in the CD-1 mouse after cross-foster and restricted gestational exposures. *Toxicological sciences : an official journal of the Society of Toxicology* **95**(17098816), 462-473.
- York, R. G., Kennedy Jr, G. L., Olsen, G. W. and Butenhoff, J. L. (2010). Male reproductive system parameters in a two-generation reproduction study of ammonium perfluorooctanoate in rats and human relevance. *Toxicology* **271**(1-2), 64-72, 10.1016/j.tox.2010.03.005.

1
2
3 Zaldivar Comenges, J.-M., Wambaugh, J. and Judson, R. (2012). Modeling In Vitro Cell-Based
4 Assays Experiments: Cell Population Dynamics. In *Models of the Ecological Hierarchy From*
5 *Molecules to the Ecospher* (F. Jordán and S. E. Jørgensen, Eds.), pp. 51-71. Elsevier.
6 Zhang, X., Diamond, M. L., Ibarra, C. and Harrad, S. (2009). Multimedia Modeling of
7 Polybrominated Diphenyl Ether Emissions and Fate Indoors. *Environmental Science &*
8 *Technology* **43**(8), 2845-2850, 10.1021/es802172a.
9
10
11
12
13
14
15
16
17
18
19
20
21
22
23
24
25
26
27
28
29
30
31
32
33
34
35
36
37
38
39
40
41
42
43
44
45
46
47
48
49
50
51
52
53
54
55
56
57
58
59
60

Tables

Table 1 PFOA *in vivo* Toxicity Studies

Study	Subject	Dose mg/kg/day	Exposure	NOEL mg/kg/day	LOEL mg/kg/day	Critical Effect
Liver						
Butenhoff <i>et al.</i> (2002), Butenhoff <i>et al.</i> (2004b)	Monkey (M) Cynomolgus	3, 10, 30/20	26 weeks Oral capsule	NA	3	Increased liver weight
Perkin <i>et al.</i> (2004)	Rat (M) ChR-CD	0.06, 0.64, 1.94, 6.50	13 weeks Diet	0.06	0.64	Increased absolute and relative liver weight, hepatic hypertrophy- reversible following 8 week recovery period
Butenhoff <i>et al.</i> (2004a), York <i>et al.</i> (2010)	Rat (M) Sprague- Dawley	1, 3, 10, 30	6 week pre mating- mating Oral gavage	NA	1	Increased absolute and relative liver weight
White <i>et al.</i> (2009), Wolf <i>et al.</i> (2007)	Mouse (F) CD-1	5, 20	GD7-17 GD10-17 GD13-17 GD15-17 Oral gavage	Maternal: NA	Maternal:5	Maternal all groups except 5(15-17): Increased relative liver weight
White <i>et al.</i> (2009), Wolf <i>et al.</i> (2007)	Mouse (F) CD-1	3, 5	GD1-17 Oral gavage	Maternal: NA	Maternal: 3	Maternal: Increased absolute and relative liver weight
DeWitt <i>et al.</i> (2008)	Mouse (F) C57BL/6N	3.75, 7.5, 15, 30	15 days Drinking water	NA	3.75	Increased relative liver weight
Developmental						
Lau <i>et al.</i> (2006)	Mouse (F) CD-1	1, 3, 5, 10, 20, 40	GD1-17 Oral gavage	Maternal: NA Developm ental: NA	Maternal: 1 Developm ental: 1	Maternal-Increased liver weight Developmental-Accelerated sexual maturity in males
White <i>et al.</i> (2009), Wolf <i>et al.</i> (2007)	Mouse (F) CD-1	5 (all but GD15-17 group), 20 (GD15-17 group only)	GD7-17 GD10-17 GD13-17 GD15-17 Oral gavage	Maternal: NA	Maternal: 5	Maternal all groups except 5 (15-17): Increased relative liver weight 20 GD15-17: Decreased pup survival
				Developm ental: NA	Developm ental: 5	Developmental all groups: Increased relative liver weight, delayed mammary gland development at PND29 and PND32 5(GD7-17, 10-17): Delayed eye opening and body hair growth
White <i>et al.</i> (2009), Wolf <i>et al.</i>	Mouse (F) CD-1	3, 5	GD1-17 Oral gavage	Maternal: NA	Maternal: 3	Maternal: Increased absolute and relative liver weight

Study	Subject	Dose mg/kg/day	Exposure	NOEL mg/kg/day	LOEL mg/kg/day	Critical Effect
(2007)			Cross-foster at birth	Developmental: NA	Developmental: 3	Developmental 3U+L, 5U, 5U+L: Delayed eye opening and hair growth PND 22-all groups: Increased relative liver weight PND22-all except 3L: Delayed mammary gland development PND42 all except 3U+L: Delayed mammary gland development PND 63all groups: Delayed mammary gland development
						Immunological
DeWitt <i>et al.</i> (2008)	Mouse (F) C57BL/6N	0, 3.75, 7.5, 15, 30	15 days Drinking water	NA	3.75	Reduced SRBC-specific IgM antibody titers

NA= not applicable/could not be determined; M = male; F= female; GD = gestation day; LD= lactation day; PND = post natal day; U= in utero exposure; L= lactational exposure; U+L= *in utero* and lactational exposure; SRBC = sheep red blood cells; IgM = immunoglobulin M

Table 2 PFOS *in vivo* Toxicity Studies

Study	Subject	Dose mg/kg/day	Exposure	NOEL mg/kg/day	LOEL mg/kg/day	Critical Effect
Liver						
Curran <i>et al.</i> (2008)	Rat (M) Sprague-Dawley 15 / group	0.14, 1.33, 3.21, 6.34	28 days, feed	0.14	1.33	Increased final relative (to BW) liver weight; decreased serum total T4
Curran <i>et al.</i> (2008)	Rat (F) Sprague-Dawley 15 / group	0.15, 1.43, 3.73, 7.58	28 days, feed	NA	0.15	Increased final relative (to BW) liver weight
Seacat <i>et al.</i> (2003)	Rat (M) Crl:CD(SD) IGS BR 5 / group	0.035, 0.14, 0.35, 1.4	98 days, feed	0.14	0.35	Centrilobular hepatic hypertrophy (at 1.4 mg/kg/day increased absolute/relative liver wt and ALT)
Seacat <i>et al.</i> (2003)	Rat (F) Crl:CD(SD) IGS BR 5 / group	0.038, 0.15, 0.38, 1.56	98 days, feed	0.38	1.56	Centrilobular hepatic hypertrophy and increased relative liver wt
Seacat <i>et al.</i> (2002)	Monkey (MF) Cynomolgus 6 / sex / group	0.03, 0.15, 0.75	182 days, oral capsule	0.15	0.75	Increased absolute and relative hepatic wt; centrilobular or diffuse hepatocellular hypertrophy
Thyroid						
Chang <i>et al.</i> (2008)	Rat (F) Sprague-Dawley 5-15 / group	15	Single oral dose	NA	15	Decreased total T4 at 2, 6 and 24 hrs Decreased total T3 and rT3 at 24 hrs Increased free T4 at 2 and 6 hrs; normal at 24 hrs
Curran <i>et al.</i> (2008)	Rat (F) Sprague-Dawley 15 / group	0.15, 1.43, 3.73, 7.58	28 days, feed	0.15	1.43	Decreased total T4
Curran <i>et al.</i> (2008)	Rat (M) Sprague-Dawley 15 / group	0.14, 1.33, 3.21, 6.34	28 days, feed	0.14	1.33	Decreased total T4
Developmental						
Butenhoff <i>et al.</i> (2009), Chang <i>et al.</i> (2009)	Rat (F) Sprague-Dawley 25 / group	0, 0.1, 0.3, 1.0	GD 0- PND 20 (41 days), oral gavage	0.3	1.0	M offspring: Decreased habituation response
Lau <i>et al.</i> (2003), Thibodeaux <i>et al.</i> (2003)	Rat (F) Sprague-Dawley 16-25 / group	1, 2, 3, 5, 10	GDs 2-20 (19 days), oral gavage	1	2	Decreased pup survival and developmental delays
Luebker <i>et al.</i> (2005b)	Rat (F) Crl:CD(SD) IGS BR VAF/+	0.1, 0.4, 1.6, 3.2	63-76 days (6 wks prior to mating through gestation and lactation across 2 generations (only 0.1	0.1	0.4	Developmental delays (eye opening)

Study	Subject	Dose mg/kg/day	Exposure	NOEL mg/kg/day	LOEL mg/kg/day	Critical Effect
			and 0.4), oral gavage			
Lau <i>et al.</i> (2003)	Mouse (F) CD1	1, 5, 10, 15, 20	GD1-18, oral gavage	5	10	Decreased pup survival
						Reproductive
Luebker <i>et al.</i> (2005a)	Rat (F) Crl:CD(SD) IGS BR VAF/+	0.1, 0.4, 1.6, 3.2	63-76 days, oral gavage	0.4	1.6	Decreased F1 Reproductive outcome
Luebker <i>et al.</i> (2005b)	Rat (F) Crl:CD(SD) IGS BR VAF/+	0.4, 0.8, 1.0, 1.2, 1.6, 2.0	63-76 days, oral gavage	1.2	1.6	Decreased viability
Chen <i>et al.</i> (2012)	Rat (F) Sprague- Dawley 10 / group	0.1, 2	GD1-2, oral gavage	0.1	2.0	Histopathological changes to lungs; Increased mortality
						Immunological
Dong <i>et al.</i> (2009)	Mouse (M) B6C3F1	0.0083, 0.083, 0.42, 0.83, 2.08	60 days, oral gavage	0.008	0.083	Increased splenic natural killer cell activity
Peden- Adams <i>et al.</i> (2008)	Mouse (M) B6C3F1	0.00018, 0.0018 0.0036, 0.018, 0.036, 0.18	28 days, oral gavage	0.00018	0.0018	Suppressed SRBC plaque- forming cell response
Peden- Adams <i>et al.</i> (2008)	Mouse (F) B6C3F1	0.00018, 0.0018 0.0036, 0.018, 0.036, 0.18	28 days, oral gavage	0.0018	0.0036	Suppressed SRBC plaque- forming cell response

BW = body weight; T4 = Thyroxine; T3 = Triiodothyronine; rT3 = reverse Triiodothyronine; ALT = Alanine Aminotransferase; F1 = first filial generation; SRBC = sheep red blood cells

Table 3 PFOA *in vivo* PK Studies

Study	Subject	Dose Regimen
Butenhoff, <i>et al.</i> (2004a)	Monkey (M) Cynomolgus	7, 10, or 12 weeks (20 mg/kg/day only) 26 weeks (all doses) of daily oral doses
Butenhoff, <i>et al.</i> (2004b)	Monkey (M/F) Cynomolgus	Single <i>iv</i> dose (10 mg/kg)
Kemper (2003)	Rat (M) Sprague- Dawley	Single <i>iv</i> dose (1 mg/kg) or oral dose (0.1, 1, 5, 25 mg/kg)
Kemper (2003)	Rat (F) Sprague- Dawley	Single <i>iv</i> dose (1 mg/kg) or oral dose (0.1, 1, 5, 25 mg/kg)
Lou, <i>et al.</i> (2009), Lau, <i>et al.</i> (unpublished)	Mouse (F) CD1	Single oral dose (1, 10, or 60 mg/kg) or 17 day repeated oral dose (20 mg/kg/day) or 29 day repeated oral dose (0.1, 1, or 20 mg/kg/day)
DeWitt, <i>et al.</i> (unpublished)	Mouse (F) C57Bl/6	28 days of daily oral doses (0.94, 1.88, 3.75, or 7.5 mg/kg/day)

Table 4 PFOS *in vivo* PK Studies

Study	Subject	Dose Regimen
Chang, <i>et al.</i> (2012)	Monkey (M/F) Cynomolgus	Single <i>iv</i> dose (2 mg/kg)
Seacat, <i>et al.</i> (2002)	Monkey (M/F) Cynomolgus	Repeated daily oral dose (0.03, 0.15, or 0.75 mg/kg/day) for 182 days
Chang, <i>et al.</i> (2012)	Rat (M/F) Sprague- Dawley	Single oral or <i>iv</i> dose (2 or 4.2 mg/kg) and oral only at 15 mg/kg
Chang, <i>et al.</i> (2012)	Mouse (M/F) CD1	Single oral dose (1 or 20 mg/kg)

Table 5 Description of Active *in vitro* Assays Common to PFOS and PFOA

Assay Name	Technology	Description	Reference
NVS_ENZ_hBACE	NovaScreen cell-free	In this assay the test chemical inhibits enzyme activity on control substrate. Beta-secretase 1 is a membrane-bound, aspartic acid protease that cleaves the amyloid precursor protein (APP) to produce the amyloid-beta peptide fragment linked as a causative factor in Alzheimer's disease. Interestingly, many of the known small molecule inhibitors of BACE being developed for the treatment of Alzheimer's are also perfluorinated compounds.	(Vassar <i>et al.</i> , 2009)
NVS_ENZ_hTie2	NovaScreen cell-free	In this assay the test chemical inhibits enzyme activity on control substrate. The TIE2 receptor tyrosine kinase binds Angiopoietin 1, required for normal blood vessel formation (angiogenesis). Angiopoietin-1 released from mural cells controls their interaction with endothelial cells and stabilization of the vasculature through binding to the TIE2 receptor.	(Kleinstreuer, <i>et al.</i> , 2011; Knudsen and Kleinstreuer, 2011)
ATG_PXRE_CIS	Attagene mammalian 2-hybrid, GAL4	In this assay the test chemical stimulates reporter gene expression controlled by pregnane X receptor response element. The PXRE binds the ligand-activated pregnane X receptor in response to a wide array of xenobiotic and endogenous compounds and subsequently regulates the expression of a number of genes of important phase I and phase II detoxification enzymes.	(Martin, <i>et al.</i> , 2010)

Table 6: Estimated and Assumed PK Parameters for the Modified Andersen, *et al.* (2006) Model for PFOA.

		CD1 Mouse (F)	C57Bl/6 Mouse (F)	Sprague-Dawley Rat (F)	Sprague-Dawley Rat (M)	Cynomolgus Monkey (M/F)	Species / Strain and Gender
		Lou, <i>et al.</i> (2009)	DeWitt, <i>et al.</i> (unpublished)	Kemper (2003)	Kemper (2003)	Butenhoff, <i>et al.</i> (2004)	Data Set Modeled
Parameter	Units						
BW	kg	0.02	0.02	0.20 (0.16 – 0.23) ^a	0.24 (0.21 – 0.28) ^a	7 (m) 4.5 (f)	
Cardiac Output ^b	L/h/kg ^{0.74}	8.68	8.68	12.39	12.39	19.8	
k _a	1/h	290 (0.6 – 73000)	340 (0.53 – 69000)	1.7 (1.1 – 3.1)	1.1 (0.83 – 1.3)	230 (0.27 – 73000)	
V _{cc}	L/kg	0.18 (0.16 – 2.0)	0.17 (0.13 – 2.3)	0.14 (0.11 – 0.17)	0.15 (0.13 – 0.16)	0.4 (0.29 – 0.55)	
k ₁₂	1/h	0.021 (3.1x10 ⁻¹⁰ – 3.8x10 ⁻⁴)	0.35 (0.058 – 52)	0.098 (0.039 – 0.27)	0.028 (0.0096 – 0.08)	0.0011 (2.4x10 ⁻¹⁰ – 3.5x10 ⁻⁴)	
R _{v2/v1}	Unitless	1.07 (0.26 – 5.84)	53 (11 – 97)	9.2 (3.4 – 28)	8.4 (3.1 – 23)	0.98 (0.25 – 3.8)	
T _{maxc}	M/h	4.91 (1.75 – 2.96)	2.7 (0.95 – 22)	1.1 (0.25 – 9.6)	190 (5.5 – 50000)	3.9 (0.65 – 9700)	
k _T	M	0.037 (0.0057 – 0.17)	0.12 (0.033 – 0.24)	1.1 (0.27 – 4.5)	0.092 (3.4x10 ⁻⁴ – 1.6)	0.043 (4.3x10 ⁻⁵ – 0.29)	
Free	Unitless	0.011 (0.0026 – 0.051)	0.034 (0.014 – 0.17)	0.086 (0.031 – 0.23)	0.08 (0.03 – 0.22)	0.01 (0.0026 – 0.038)	
Q _{filc}	L/h	0.077 (0.015 – 0.58)	0.017 (0.010 – 0.081)	0.039 (0.014 – 0.13)	0.22 (0.011 – 58)	0.15 (0.02 – 24)	
V _{filc}	L/kg	9.7x10 ⁻⁴ (3.34x10 ⁻⁹ – 7.21)	7.6x10 ⁻⁵ (2.7x10 ⁻¹⁰ – 6.4)	2.6x10 ⁻⁵ (2.9x10 ⁻¹⁰ – 28)	0.0082 (1.3x10 ⁻⁸ – 7.6)	0.0021 (3.3x10 ⁻⁹ – 6.9)	

Means and 95% credible interval (in parentheses) from Bayesian analysis are reported. For some parameters the distributions are quite wide, indicating uncertainty in that parameter (i.e., the predictions match the data equally well for a wide range of values). As part of the Bayesian formalism, it is the posterior distribution of parameter values, as opposed to the mean values, that is used to make the predictions in Figures 1-4.

^a Estimated average BW for species used except with Kemper (2003) study where individual rat weights were available and assumed to be constant.

^b Cardiac outputs obtained from Davies & Morris (1993)

Table 7 Estimated and assumed pharmacokinetic parameters for the modified Andersen et al. (2006) model for PFOS.

		Mouse / CD1 (F)	Mouse / CD1 (M)	Rat / Sprague-Dawley (F)	Rat / Sprague-Dawley (M)	Monkey / Cynomolgus (M/F)	Species / Strain and Gender
		Chang, <i>et al.</i> (2012)	Chang, <i>et al.</i> (2012)	Chang, <i>et al.</i> (2012)	Chang, <i>et al.</i> (2012)	Seacat, <i>et al.</i> (2002) and Chang, <i>et al.</i> (2012)	Data Set Modeled
Parameter	Units						
BW ^a	kg	0.02	0.02	0.203	0.222	3.42	
Cardiac Output ^b	L/h/kg ^{0.74}	8.68	8.68	12.39	12.39	19.8	
k _a	1/h	1.16 (0.617 - 42400)	433.4 (0.51 - 803.8)	4.65 (3.02 - 1980)	0.836 (0.522 - 1.51)	132 (0.225 - 72100)	
V _{cc}	L/kg	0.264 (0.24 - 0.286)	0.292 (0.268 - 0.317)	0.535 (0.49 - 0.581)	0.637 (0.593 - 0.68)	0.303 (0.289 - 0.314)	
k ₁₂	1/h	0.0093 (2.63e-10 - 38900)	2976 (2.8e-10 - 4.2e4)	0.0124 (3.1e-10 - 46800)	0.00524 (2.86e-10 - 43200)	0.00292 (2.59e-10 - 34500)	
R _{V2:V1}	Unitless	1.01 (0.251 - 4.06)	1.29 (0.24 - 4.09)	0.957 (0.238 - 3.62)	1.04 (0.256 - 4.01)	1.03 (0.256 - 4.05)	
T _{maxc}	M/h	57.9 (0.671 - 32000)	1.1e4 (2.1 - 7.9e4)	1930 (4.11 - 83400)	1.34e-06 (1.65e-10 - 44)	15.5 (0.764 - 4680)	
k _T	M	0.0109 (1.44e-05 - 1.45)	381 (2.6e-5 - 2.9e3)	9.49 (0.00626 - 11100)	2.45 (4.88e-10 - 60300)	0.00594 (2.34e-05 - 0.0941)	
Free	Unitless	0.00963 (0.00238 - 0.0372)	0.012 (0.0024 - 0.038)	0.00807 (0.00203 - 0.0291)	0.00193 (0.000954 - 0.00249)	0.0101 (0.00265 - 0.04)	
Q _{filc}	L/h	0.439 (0.0125 - 307)	27.59 (0.012 - 283)	0.0666 (0.0107 - 8.95)	0.0122 (0.0101 - 0.025)	0.198 (0.012 - 50.5)	
V _{filc}	L/kg	0.00142 (4.4e-10 - 6.2)	0.51 (3.5e-10 - 6.09)	0.0185 (8.2e-07 - 7.34)	0.000194 (1.48e-09 - 5.51)	0.0534 (1.1e-07 - 8.52)	

^a Average BW for species -- individual-specific BWs

^b Cardiac outputs obtained from Davies & Morris (1993)

Table 8 Transition Regions for Each Category of Toxicity for PFOA *in vivo* Studies

	Transition to Observed Effect (µM)			
	Union		Intersect	
Endpoint	Lower	Upper	Lower	Upper
All	0.409 ^a	270.97	8.504	40.861
Liver	0.409 ^a	270.97	8.504	40.861
Developmental	0.973 ^a	217.51	1.738 ^a	97.307
Immunological ^b	1.297 ^a	165.98	1.297 ^a	129.66

^aIn studies without a NOEL, LOEL/100 was assumed.

^bThere was only one PFOA immunological study, so the union and intersect are equivalent.

Table 9 Transition Regions for Each Category of Toxicity for PFOS *in vivo* Studies

	Transition to Observed Effect (µM)			
	Union		Intersect	
Endpoint	Lower	Upper	Lower	Upper
All	0.014 ^a	629.52	conflict ^b	
Liver	0.065 ^a	190.26	conflict ^b	
Thyroid	0.456 ^a	70.375	7.39	45.38
Developmental	9.589	629.52	conflict ^b	
Reproductive	3.317	211.34	conflict ^b	
Immunological	0.014	14.967	conflict ^b	

^aIn studies without a NOEL, LOEL/100 was assumed.

^bCalculated exposures for one outlier study produced conflicting NOELs and LOELs so that no intersecting (common to all studies) transition region was identified.

Table 10 PFOA *in vitro* Assay Results in Order of 50% Activation Concentration (AC₅₀).

	Assay Name	Assay Type	AC ₅₀ (μM)	E _{max}	E _{max} Cutoff	All	Liver	In Vivo Coincidence		In Vivo Toxicity Signature				PFOS Hit
								Developmental	Immunological	Rat Reproductive	Rat Developmental	Rabbit Developmental	Vascular Disruptor	
1	BSK_SM3C_SAA_up	Cell-based	2.73	1.26	1.21	W	W	S	S					
2	NVS_ENZ_hBACE	Cell-free	3.55	83.7	30	W	W	S	S					Y
3	BSK_3C_uPAR_down	Cell-based	5.45	1.42	1.4	W	W	S	S				+	
4	NVS_GPCR_hORL1	Cell-free	5.56	102	30	W	W	S	S		+			
5	NVS_ENZ_hTie2	Cell-free	15.2	58.6	30	S	S	S	S				+	Y
6	ATG_PPARGa_TRANS_perc	Cell-based	37.7	102	2	S	S	S	S	+				
7	ATG_PPARGa_TRANS_perc	Cell-based	39.6	48.9	2	S	S	S	S	+				
8	ATG_PXRE_CIS_perc	Cell-based	42.8	49.5	2	W	W	S	S	+				Y
9	ATG_ERE_CIS_perc	Cell-based	48.3	62.1	2	W	W	S	S	+			+	
10	ATG_NRF2_ARE_CIS_perc	Cell-based	50.9	53.7	2	W	W	S	S					
11	ATG_PPARGb_TRANS_perc	Cell-based	53.1	86.7	2	W	W	S	S	+				
12	ATG_ERa_TRANS_perc	Cell-based	53.2	110	2	W	W	S	S				+	

“S” indicates strong coincidence of *in vitro* activity with the toxicity transition region of the *in vivo* studies (intersect), while “W” indicates weak coincidence (union). “+” indicates that that assay is part of an *in vitro* signature of toxicity. Assays are numbered in the same order listed on the right-hand side of Figure 5.

Table 11 Redacted PFOS *in vitro* Assay Results in Order of 50% Activation Concentration (AC₅₀).

						In Vivo Coincidence					In Vivo Toxicity Signature					
Assay Name		Assay Type	AC ₅₀ (μM)	E _{max}	E _{max} Cutoff	All	Liver	Thyroid	Developmental	Reproductive	Immunological	Rat	Rat	Rabbit	Vascular	PFOA Hit
1	NVS_ADME_hCYP2C9	Cell-free	0.0236	87.3	30	W					W					
2	NVS_ADME_rCYP2C11	Cell-free	0.0557	99.2	30	W					W	+				
3	NVS_ENZ_hBACE	Cell-free	0.361	98.6	30	W	W				W					Y
4	NVS_ADME_hCYP2C18	Cell-free	0.676	77.1	30	W	W	W			W					
5	NVS_ENZ_hPTPN11	Cell-free	0.787	57.3	30	W	W	W			W				+	
8	NVS_NR_rAR	Cell-free	3.14	67.8	30	W	W	W			W	+				
9	NVS_ENZ_hTie2	Cell-free	4.65	99.6	30	W	W	W		W	W				+	Y
12	NVS_GPCR_hAdra2C	Cell-free	6.33	79.8	30	W	W	W		W	W	+				
18	NVS_NR_hAR	Cell-free	11.6	68.1	30	W	W	S	W	W	W	+				
34	BSK_BE3C_PA11_down	Cell-based	20.1	1.5	1.5	W	W	S	W	W					+	
35	NVS_ENZ_hPTPN12	Cell-free	22.1	97.9	30	W	W	S	W	W					+	
37	ATG_PXRE_CIS_perc	Cell-based	23.3	105	2	W	W	S	W	W		+				Y
52	NVS_GPCR_h5HT6	Cell-free	30.1	69.9	30	W	W	S	W	W		+				

“S” indicates strong coincidence of *in vitro* activity with the toxicity transition region of the *in vivo* studies (intersect), while “W” indicates weak coincidence (union). “+” indicates that that assay is part of an *in vitro* signature of toxicity. Assays are numbered in the same order listed on the right-hand side of Figure 6. Only those assays active in one of the toxicity signatures or also found for PFOA are shown – the full list of active assays is available in Supplemental Table 9.

Figure Captions

Figure 1 Distribution of ToxCast *in vitro* activity for PFOS (left) and PFOA (right). The concentration-response curves for all of these assays were successfully described by a Hill equation and are therefore putative “hits”. The varying assay activities have different acceptability cutoffs for efficacy; for comparison purposes all assays have been scaled by their respective acceptability cutoffs (e.g. fold change above background). The dotted line (at scaled efficacy = 1) indicates where this scaled cutoff occurs.

Figure 2 Andersen *et al.* (2006) PK model with oral absorption. A_{gut} is the amount of chemical in the gut; k_a is the first order rate constant for absorption from the gut; Q_{fil} is the flow through the filtrate compartment; C_1, C_2 , and C_3 are the chemical concentrations in the central, second, and filtrate compartments, respectively; V_c , V_t , and V_{fil} are the volumes of distribution of the central, second, and filtrate compartments; F_{free} is the free fraction of compound in the central compartment; Q_d is the flow between the central and second compartments; the saturable resorption process from the filtrate back into the central compartment is modeled with Michaelis-Menten kinetics, with a maximum rate T_{maximum} and a half-maximum concentration K_T .

Figure 3 Concordance of measured and predicted final serum concentration for the *in vivo* toxicity studies that measured serum concentration at the termination of the study for PFOS (left) and PFOA (right). Only the monkey data (Butenhoff, *et al.*, 2004a; Butenhoff, *et al.*, 2004b) was used for estimating PK model parameters.

Figure 4 Consistency of predicted dose metrics across various *in vivo* toxicity studies for PFOS (left) and PFOA (right). All metrics have been normalized by taking the difference from the mean value and dividing by the mean. Original units for administered dose were either mg/kg BW or mg/kg BW/day.

Figure 5 Average serum concentration during PFOA *in vivo* toxicity studies and *in vitro* activities. Box and whisker plots indicate median, mean \pm standard deviation, and 95% credible intervals for LOEL and NOEL (lower of two points when NOEL was observed). Credible intervals are calculated using the distribution of PK model parameters for the animal and dose regimen used in each *in vivo* study. The shaded region between LOEL and NOEL indicates toxicity transition region. Horizontal bars indicate the ToxCast PFOA *in vitro* AC50s (concentrations) from Figure 1 for cell-based (solid) and binding (dashed) assays. The horizontal bars are plotted translucently, so that denser lines indicate multiple active assays. Black boxes indicate benchmark doses, which could be calculated for three studies only. The *in vitro* assay AC50s are numbered in order of potency starting at 1 (most potent), as in Table 10.

Figure 6 Average serum concentration during PFOS *in vivo* toxicity studies and *in vitro* activities. Box and whisker plots indicate median, mean \pm standard deviation, and 95% credible intervals for LOEL and NOEL (lower of two points when NOEL was observed). Credible intervals are calculated using the distribution of PK model parameters for the animal and dose regimen used in each *in vivo* study. The shaded region between LOEL and NOEL indicates toxicity transition region. Horizontal bars indicate the ToxCast PFOS *in vitro* AC50s (concentrations) from Figure 1 for cell-based (solid) and binding (dashed) assays. The horizontal bars are plotted translucently, so that denser lines indicate multiple active assays. The *in vitro* assay AC50s are numbered in order of potency starting at 1 (most potent), as in Table 11.

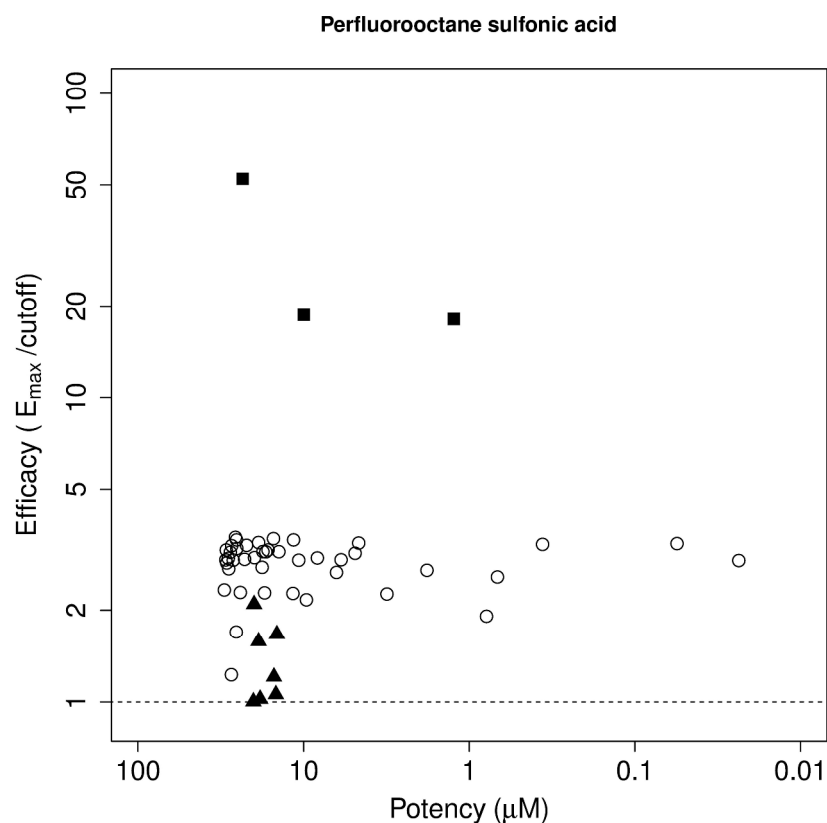


Figure 1 Distribution of ToxCast in vitro activity for PFOS (left) and PFOA (right). The concentration-response curves for all of these assays were successfully described by a Hill equation and are therefore putative "hits". The varying assay activities have different acceptability cutoffs for efficacy; for comparison purposes all assays have been scaled by their respective acceptability cutoffs (e.g. fold change above background). The dotted line (at scaled efficacy = 1) indicates where this scaled cutoff occurs.

279x361mm (300 x 300 DPI)

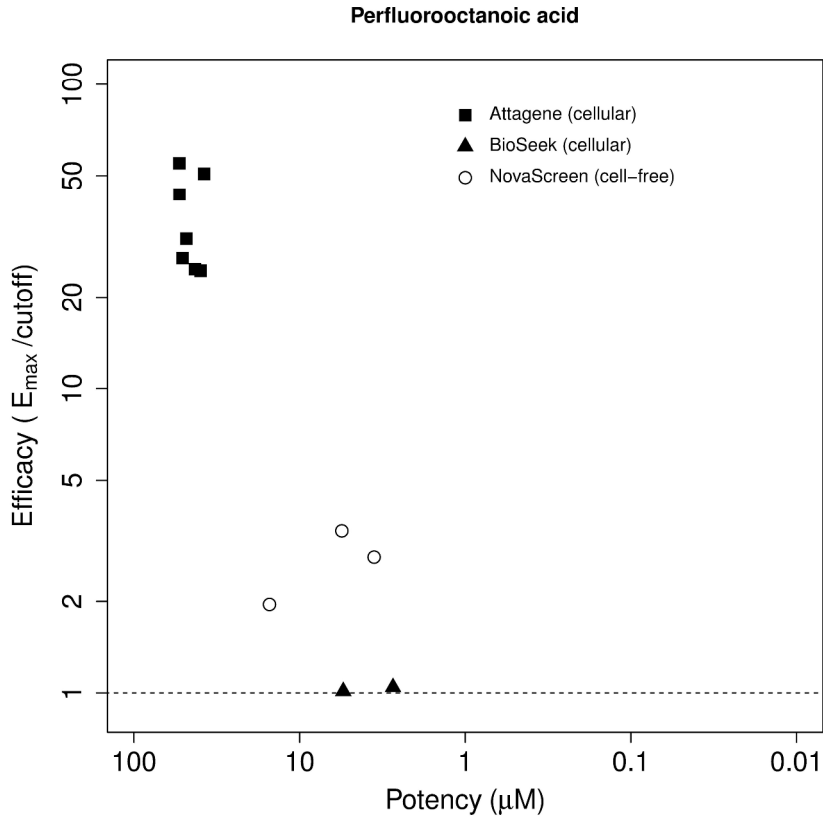


Figure 1 Distribution of ToxCast in vitro activity for PFOS (left) and PFOA (right). The concentration-response curves for all of these assays were successfully described by a Hill equation and are therefore putative “hits”. The varying assay activities have different acceptability cutoffs for efficacy; for comparison purposes all assays have been scaled by their respective acceptability cutoffs (e.g. fold change above background). The dotted line (at scaled efficacy = 1) indicates where this scaled cutoff occurs.

279x361mm (300 x 300 DPI)

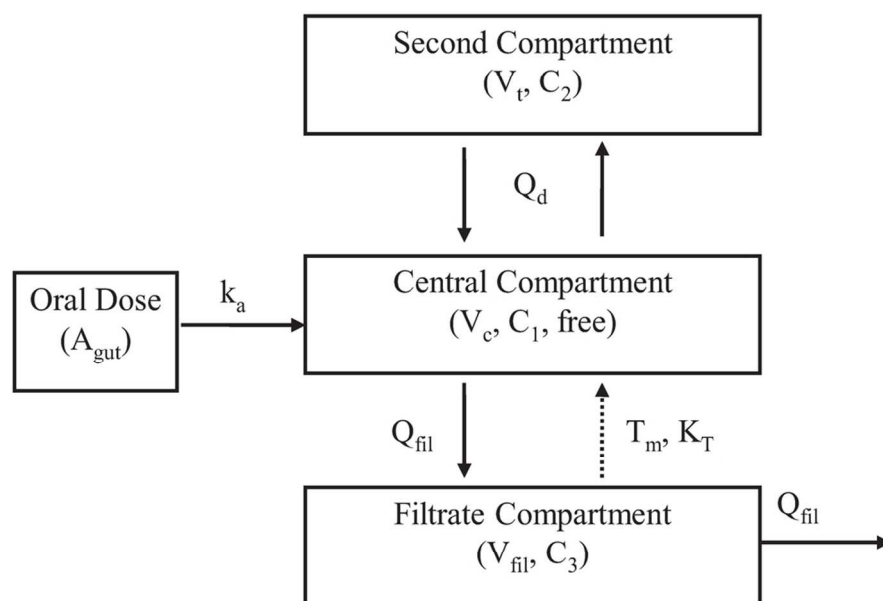


Figure 2 Andersen et al. (2006) PK model with oral absorption. A_{gut} is the amount of chemical in the gut; k_a is the first order rate constant for absorption from the gut; Q_{fil} is the flow through the filtrate compartment; C_1, C_2 , and C_3 are the chemical concentrations in the central, second, and filtrate compartments, respectively; V_c, V_t , and V_{fil} are the volumes of distribution of the central, second, and filtrate compartments; Free is the free fraction of compound in the central compartment; Q_d is the flow between the central and second compartments; the saturable resorption process from the filtrate back into the central compartment is modeled with Michaelis-Menten kinetics, with a maximum rate T_{maximum} and a half-maximum concentration K_T .

101x67mm (300 x 300 DPI)

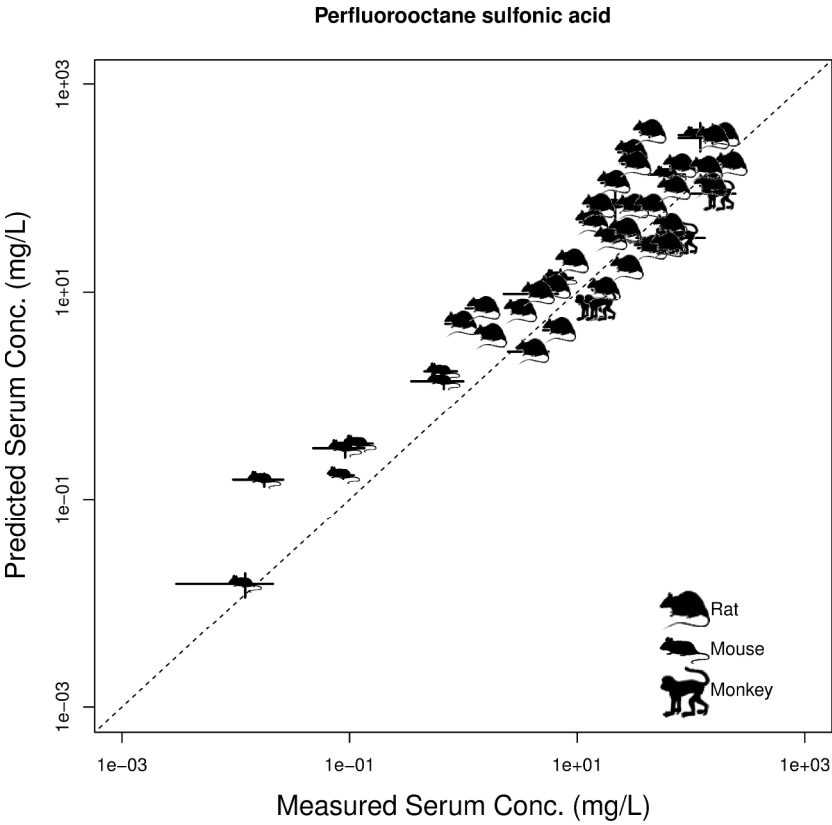


Figure 3 Concordance of measured and predicted final serum concentration for the in vivo toxicity studies that measured serum concentration at the termination of the study for PFOS (left) and PFOA (right). Only the monkey data (Butenhoff, et al., 2004a; Butenhoff, et al., 2004b) was used for estimating PK model parameters.

279x361mm (300 x 300 DPI)

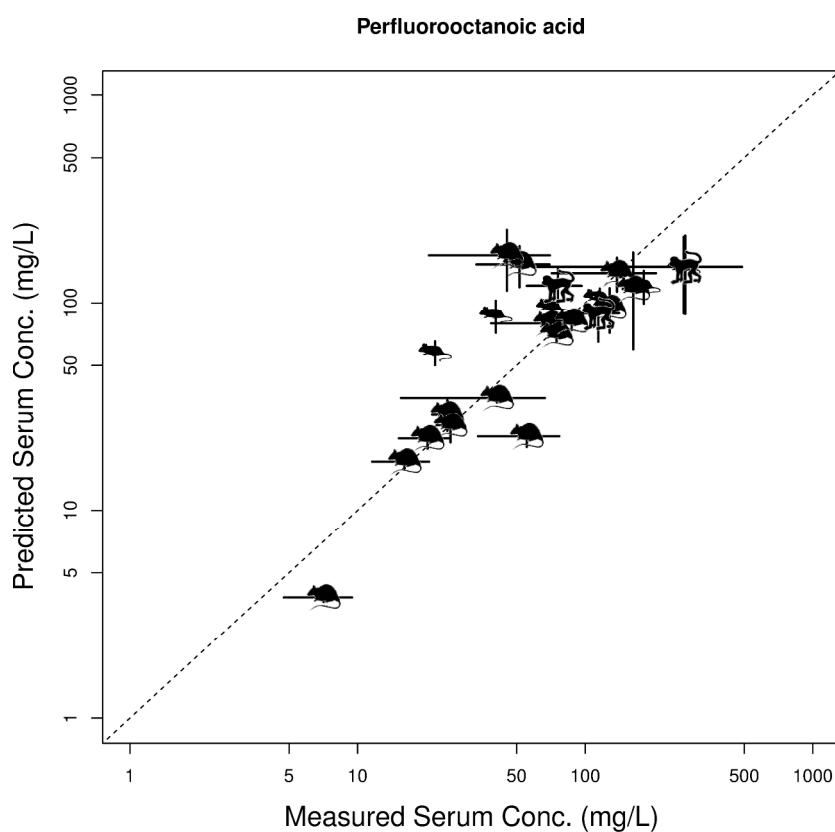


Figure 3 Concordance of measured and predicted final serum concentration for the in vivo toxicity studies that measured serum concentration at the termination of the study for PFOS (left) and PFOA (right). Only the monkey data (Butenhoff, et al., 2004a; Butenhoff, et al., 2004b) was used for estimating PK model parameters.

279x361mm (300 x 300 DPI)

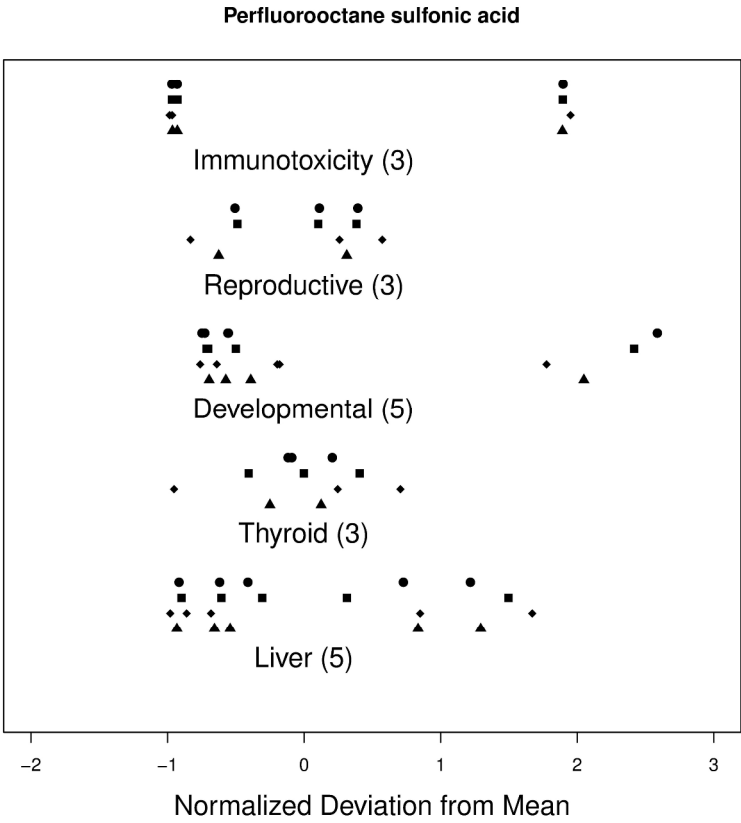


Figure 4 Consistency of predicted dose metrics across various in vivo toxicity studies for PFOS (left) and PFOA (right). All metrics have been normalized by taking the difference from the mean value and dividing by the mean. Original units for administered dose were either mg/kg BW or mg/kg BW/day.
279x361mm (300 x 300 DPI)

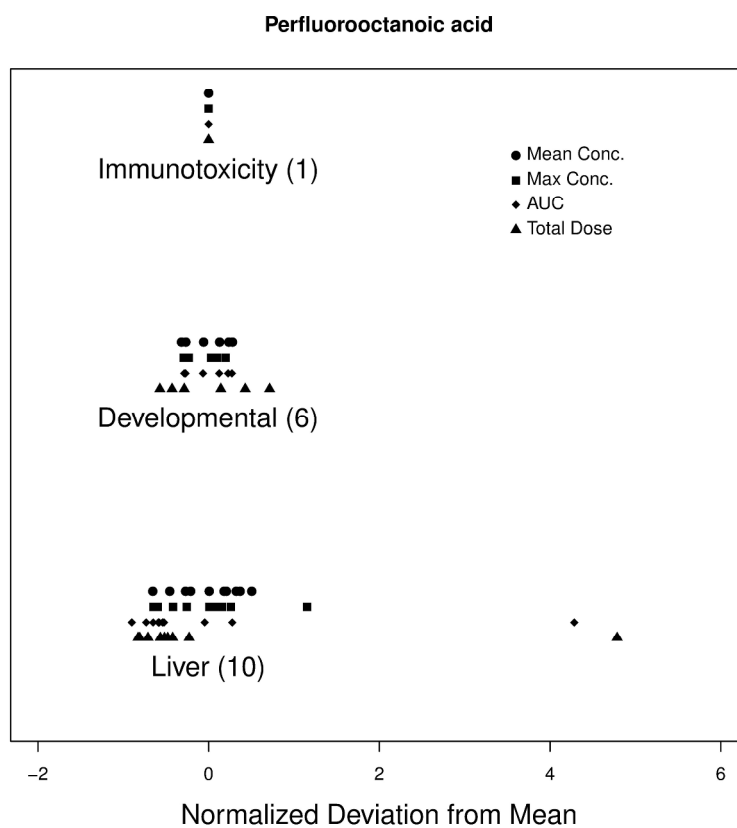


Figure 4 Consistency of predicted dose metrics across various in vivo toxicity studies for PFOS (left) and PFOA (right). All metrics have been normalized by taking the difference from the mean value and dividing by the mean. Original units for administered dose were either mg/kg BW or mg/kg BW/day.
279x361mm (300 x 300 DPI)

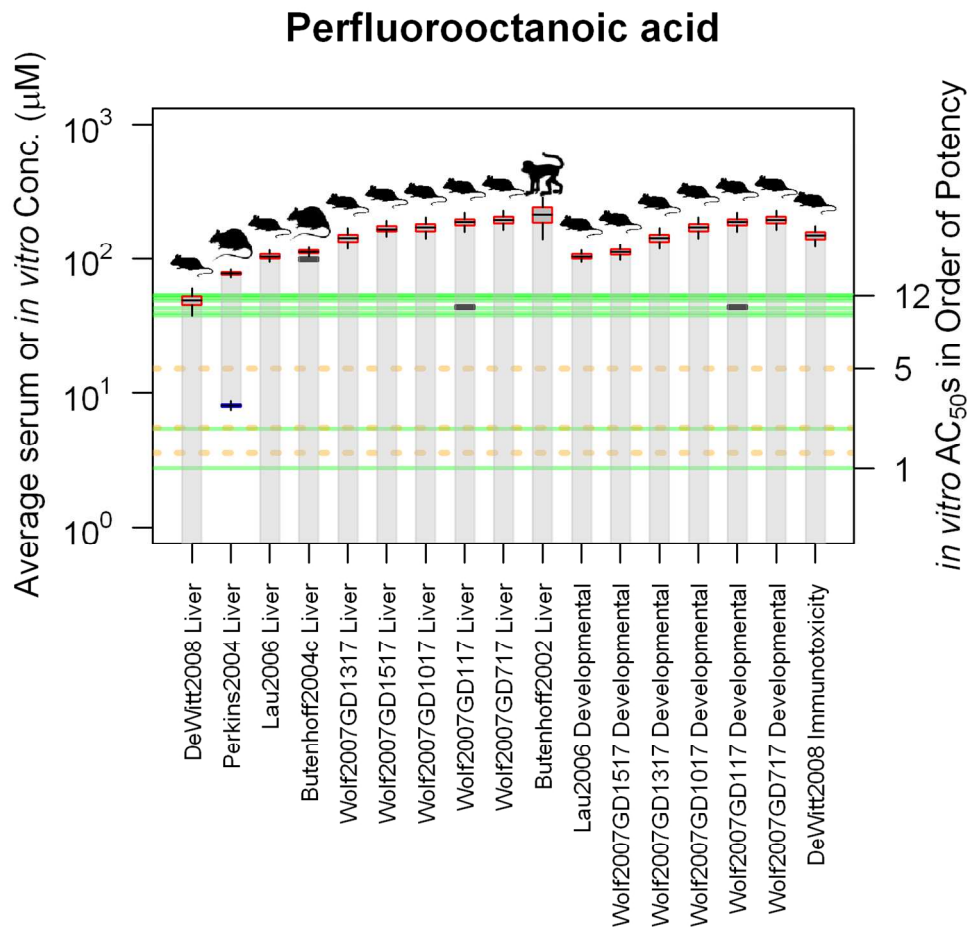


Figure 5 Average serum concentration during PFOA *in vivo* toxicity studies and *in vitro* activities. Box and whisker plots indicate median, mean \pm standard deviation, and 95% credible intervals for LOEL and NOEL (lower of two points when NOEL was observed). Credible intervals are calculated using the distribution of PK model parameters for the animal and dose regimen used in each *in vivo* study. The shaded region between LOEL and NOEL indicates toxicity transition region. Horizontal bars indicate the ToxCast PFOA *in vitro* AC₅₀s (concentrations) from Figure 1 for cell-based (solid) and binding (dashed) assays. The horizontal bars are plotted translucently, so that denser lines indicate multiple active assays. Black boxes indicate benchmark doses, which could be calculated for three studies only. The *in vitro* assay AC₅₀s are numbered in order of potency starting at 1 (most potent), as in Table 10.

127x127mm (300 x 300 DPI)

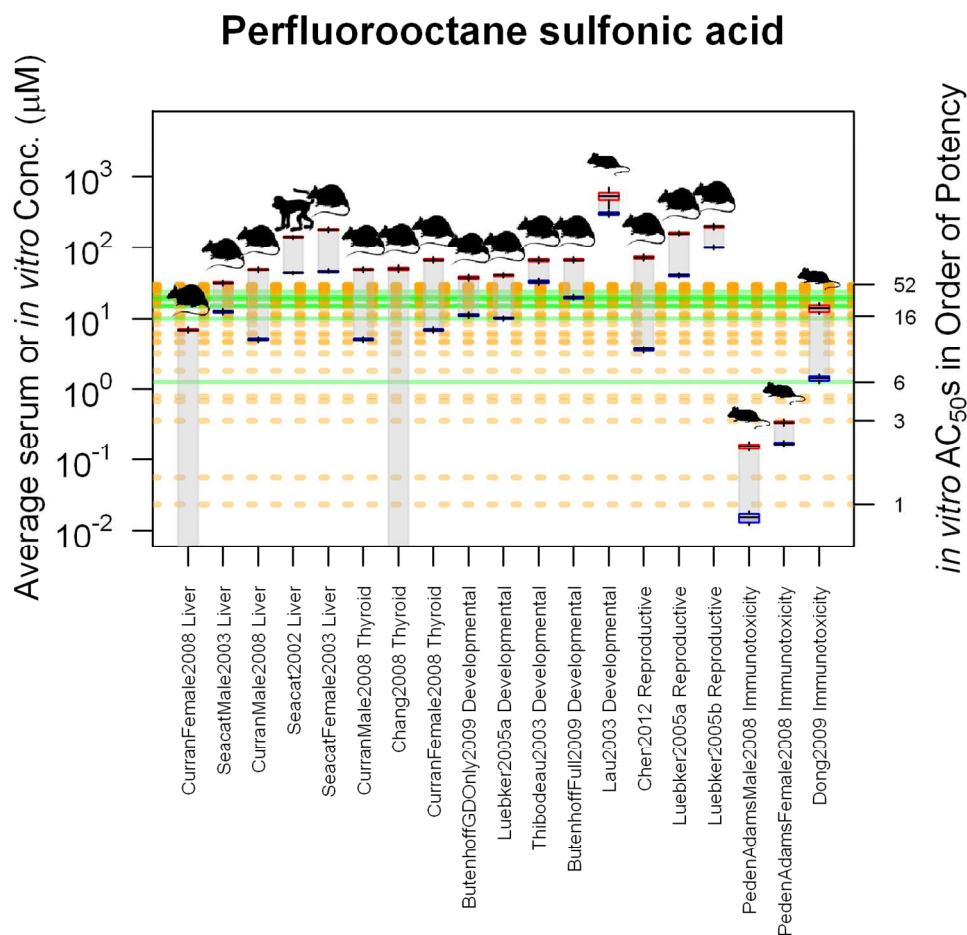


Figure 6 Average serum concentration during PFOS *in vivo* toxicity studies and *in vitro* activities. Box and whisker plots indicate median, mean \pm standard deviation, and 95% credible intervals for LOEL and NOEL (lower of two points when NOEL was observed). Credible intervals are calculated using the distribution of PK model parameters for the animal and dose regimen used in each *in vivo* study. The shaded region between LOEL and NOEL indicates toxicity transition region. Horizontal bars indicate the ToxCast PFOS *in vitro* AC₅₀s (concentrations) from Figure 1 for cell-based (solid) and binding (dashed) assays. The horizontal bars are plotted translucently, so that denser lines indicate multiple active assays. The *in vitro* assay AC₅₀s are numbered in order of potency starting at 1 (most potent), as in Table 11.

127x127mm (300 x 300 DPI)